Organic Polymers for Triggering Cell Death in Cancer Cells

by

Fatma ÖZ

A Dissertation Submitted to the
Graduate School of Sciences and Engineering
in Partial Fulfillment of the Requirements for
the Degree of

Master of Science

in

(Biomedical Sciences and Engineering)

August 9, 2022

Organic Polymers for Triggering Cell Death in Cancer Cells

Koç University

Graduate School of Sciences and Engineering

This is to certify that I have examined this copy of a master's thesis by

Fatma Öz

and have found that it is complete and satisfactory in all respects,
and that any and all revisions required by the final
examining committee have been made.

Committee Members:

Prof. Özlem Yalçın (Advisor)

Prof. Sacit Karamürsel

Asst. Prof. Ahmet Can Erten

Date: August 9, 2022

[To Nilgül and Yaşar ÖZ]

ABSTRACT

Organic Polymers for Triggering Cell Death in Cancer Cells

Fatma Öz

Master of Science in Biomedical Sciences and Engineering

August 9, 2022

Organic polymers are promising candidates for semiconductor-cell interfaces due to their advantages, such as lightness, biocompatibility, and flexibility. Especially, hybrid interfaces bear a significant potential to regulate cell activities. Photoelectrical stimulation of cancer cells using organic polymers has shown a promising future in cell death. However, long treatment duration may be disadvantageous. In this respect, this thesis is focused on the effect of increasing photocurrent level using P3HT (poly(3-hexylthiophene2,5-diyl)): $PC_{70}BM$ ([6,6]-phenyl-C71-butyric acid methyl ester) to decrease treatment duration. Moreover, we are interested in the impact level of different parameters such as polymer concentration, frequency, and light intensity to induce cell death. This work examines the first-time opportunity to use a hybrid biointerface for cell death in A375-P and MDA-MB-231 cell lines.

First, polymer concentration was optimized to increase photocurrent produced by photoelectrode. Subsequently, the proper extracellular matrix (ECM) was tested to provide the best cell dynamics. Trypan blue counting indicated that cell viability has decreased in the presence of photocurrent. Flow cytometry results proved the activation of Annexin-V and Propidium Iodide, which demonstrates apoptosis/necrosis, has the highest percentage toward photocurrent. Further, Live Cell Imaging allowed us to analyze

calcium signaling to understand death pathways. We studied the reactive oxygen species (ROS) production of substrates to evaluate toxicity.

Altogether, the experimental results reported in this thesis may be useful for the *in vivo* experiments and future characterization of potential devices.

ÖZETÇE

Kanser Hücrelerinde Hücre Ölümünü Tetiklemek için Organik Polimerler

Fatma Öz

Biyomedikal Bilimler ve Mühendislik, Yüksek Lisans

Ağustos 9, 2022

Organik polimerler, hafiflik, biyouyumluluk ve esneklik gibi avantajları nedeniyle yarı iletken hücre arayüzleri için umut verici adaylardır. Özellikle hibrit arayüzler, hücre aktivitelerini düzenlemek için önemli bir potansiyele sahiptir. Organik polimerler kullanılarak kanser hücrelerinin fotoelektrik uyarımı, hücre ölümünde önemlidir. Ancak uzun tedavi süresi dezavantajlı olabilir. Bu bağlamda, bu tez, P3HT (poli(3-heksiltiyofen2,5-diyl)): PC70BM ([6,6]-fenil-C71-butirik asit metil ester) kullanılarak fotoakım seviyesinin arttırılmasının süreyi azaltma etkisine odaklanmıştır. Ayrıca, hücre ölümünü indüklemek için polimer konsantrasyonu, frekans ve ışık yoğunluğu gibi farklı parametrelerin etki düzeyi çalışılmıştır. Bu çalışma, A375-P ve MDA-MB-231 hücre hatlarında hücre ölümü için hibrit biyo-arayüzün ilk kez kullanılması fırsatını incelemektedir.

İlk olarak, fotoelektrot tarafından üretilen foto akımı artırmak için polimer konsantrasyonu optimize edildi. Ardından, en iyi hücre dinamiklerini sağlamak için uygun ektraselüler matriks (ECM) test edildi. Tripan mavisi sayımı, fotoakım varlığında hücre canlılığının azaldığını gösterdi. Akış sitometrisi sonuçları, apoptoz/nekroz gösteren Annexin-V ve Propidium Iyodör'ün aktivasyonunun fotoakım yönünde en yüksek yüzdeye sahip olduğunu kanıtladı. Ayrıca, Canlı Hücre Görüntüleme, kalsiyum sinyalini

analiz ederek ölüm yolu hakkında fikir sahibi olmamızı sağladı. Toksisiteyi değerlendirmek için substratların reaktif oksijen türleri (ROS) üretimi incelendi.

Genel olarak, bu tezde bildirilen deneysel sonuçlar, *in vivo* deneyler ve potansiyel cihazların gelecekteki karakterizasyonu için önemli olabileceği düşünülmektedir.

ACKNOWLEDGEMENTS

Firstly, I would like to express my special thanks to my supervisor Professor Özlem Yalçın who made this work possible. I was lucky enough to have her guidance and support, especially during the pandemic.

I thank my jury committee members, Asst. Professor Ahmet Can Erten and Prof. Sacit Karamürsel for their feedback about my work and their valuable time.

I had the pleasure of working with Molecular Hematophysiology Lab members, including Evrim Göksel, Yunus Gürpınar, Elif Uğurel, Neslihan Çilek, and KUTTAM members. I owe special thanks to Evrim Göksel, so I would like to express my deepest appreciation for her professional and personal support. Many thanks to Yunus Gürpınar for his valuable contributions.

I also thank my friends from IDEALAB, Güncem Özgün Eren, Onuralp Karatüm, Rustamzhon Melikov, Asım Ünal, Rıdvan Balamur, Deniz Aktaş, and Humeyra Nur Kaleli for giving me precious memories and support. In particular, I am grateful to Şule Eren for being my friend and for her endless positive energy.

Thanks to Meryem Eren, Fatma Betül Ertem, and Minahil Khan for being there when I needed.

Words cannot express my gratitude and love for my family, especially my mother and father. This thesis would not have been possible without you. Whenever I had difficulties, you were always there to give your biggest encouragements and unconditional love. Even though I can't see you and hear your voice right now, I still feel you in my heart. I am deeply indebted to my aunt, Fatma Yıldız, and my uncle, Emil Yıldız, for being my second parents. I thank my beloved brother, Salih ÖZ, and sister, Ebru Yıldız. I am the luckiest to have all of you. You have my purest love and thank you so much for believing in me. I will always do my best to honour this big family.

I acknowledge that some of the figures were created with BioRender.com.

TABLE OF CONTENTS

LIST OF TABLES

LIST OF FIGURES

ABBREVIATIONS

Ca^{2+}	Calcium
CDKs	Cyclin-dependent kinases
ECM	Extracellular matrix
VGCC	Voltage gated calcium channels
ROS	Reactive oxygen species
PDT	Photodynamic Therapy
PTT	Photothermal Therapy
P3HT	poly(3-hexylthiophene2,5-diyl)
PC71BM	[6,6]-Phenyl-C71-butyric acid methyl ester
ITO	Indium thin oxide
DMEM	Dulbecco's Modified Eagle's Medium
PI	Propidium Iodide
H33342	Hoechst 33342
F4AM	Fluo4 AM
ZnO	Zinc oxide

Chapter 1:

INTRODUCTION

Cancer is one of the most serious diseases with fatal effects all over the world. It starts when a cell breaks free from the normal cell cycle and then continues with increasing proliferation. Notably, studies indicated that membrane potential has functional roles in cell proliferation and is consequently associated with cancer (Mazia et al., 1975; Yang & Brackenbury, 2013).

Membrane potential fluctuates after the ionic transition from extracellular to intracellular level. Calcium ions are one of the main types of ions conducted in the membrane and take significant roles ranging from cell activities to communicating (Whitaker & Patel, 1990). At the cellular level, Ca^{2+} is obtained either externally or internally. While the endoplasmic reticulum or sarcoplasmic reticulum might be classified as the internal source, ion channels can be categorized as the fundamental external sources, and the control of Ca^{2+} levels is ensured through voltage-gated ion channels (Bagur & Hajnoczky, 2017). Moreover, control of Ca^{2+} signaling might trigger various cellular functions ending up cell death. It has been indicated that overload of Ca^{2+} ions leads to necrosis or programmed cell death, called apoptosis (Berridge et al., 1998).

Although efficient cancer treatment methods are used in clinics, existing technologies incline to severe side effects. For instance, treatment duration and dose intensity in chemotherapy might lead to organ failure in the long term (Lyman, 2009). Electrical stimulation has been used in different types of tumor treatment (Janigro et al., 2006; Li et al., 2016). Besides, previous studies have shown that targeting ion channels, especially calcium channels, in cancerous cells is an impressive way to promote cell death (Phan et al., 2017).

Regulating cell activities through photoelectrical stimulation has emerged as remarkable technology in cell research to enhance novel applications. Photoinduced charges created via light illumination are crucial for activating gated ion channels and stimulating cell membranes. One of the main advances of photoelectrical stimulation is in devices that are used in the treatment of degenerative disorders, such as retinal implants. Different photovoltaic materials, including organic polymers and quantum dots, are used in these platforms to excite cell membranes and gain targeted results (Bareket-

Keren & Hanein, 2014; Feyen et al., 2016; Ghezzi et al., 2013; Vargas-Estevez et al., 2018). During photostimulation of the cell, excitons are created, paving the way to the membrane potential changes, and opening of voltage-gated ion channels. Recently, it has been shown that photoelectrical stimulation of voltage-gated calcium channels might be a novel method to treat cancer (Aria, 2021).

In this thesis, we aimed to show that increasing photocurrent levels might shorten the treatment time. At this point, the originalities of this technique are using PCBM, different light duration pulses, and intensities with various light treatment times. It has been expressed that a broad number of cancer cells have voltage-gated ion channels such as breast, prostate, cervical, and colon (Rao et al., 2015). So, we worked with two different cell lines, including MDA-MB-231(adenocarcinoma) and A-375 P(melanoma), to generalize the photocurrent effect in cell death. Photostimulation technology is expected to damage healthy cells less than traditional therapies. On the other hand, photoelectrical stimulation requires lower light intensities compared to photodynamic and photothermal therapies.

Chapter 2:

LITERATURE REVIEW

2.1 Cancer Cell, Membrane Potential and Depolarization

Various types of cancers have their specifications; however, in broad definition, cancer is uncontrollable cell division. The cell cycle is necessary to ensure vital activities such as metabolic activities, growth, reproduction, and repair (Schafer, 1998).

Mitosis is the form of the cell cycle in which the number of cells is increased by replicating genetic material. The mitotic cell cycle consists of two phases: interphase (G1, S, G2) and M phase. G1 and G2 phases are the gap phases in which cell growth and preparation occur. DNA (deoxyribonucleic acid) is replicated during S (synthesis) phase, while cell division physically happens in the M phase. The cell cycle is controlled and regulated by cyclins and cyclin-dependent kinases (CDKs) (Malumbres & Barbacid, 2009). However, the errors in checkpoints during the cell cycle may induce cancer cell accumulation (Figure 2.1).

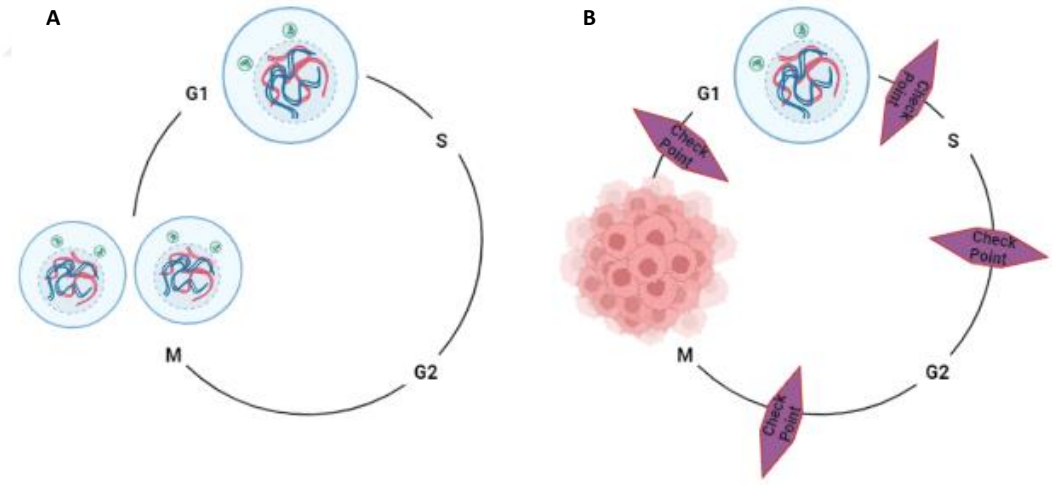

Figure 2.1: Progress of cell cycle in healthy cells (A) and cancerous cells (B).

The membrane potential is one of the critical factors that plays a role in regulating the cell cycle. Mainly, it is believed that depolarization is the key factor in DNA synthesis and mitosis (Binggeli & Weinstein, 1985; Orr et al., 1972). Initially, Cone et al. (1971) established that while hyperpolarizing Chinese hamster ovary (CHO) cells block the cell cycle, depolarizing restarts it.

Wonderlin *et al.* (1995) have recorded changes in the membrane potential of MCF-7 (adenocarcinoma) cells during cell cycle progression. It has been indicated that

membrane potential hyperpolarizes during G1/S transition due to the cell accumulation in S. Hence, depolarization of membrane potential stops G1/S progression.

In 2012, Lobikin *et al.* were able to reveal the consistent relation between increased tumor proliferation and depolarized membrane potential by *in vivo* studies of Xenopus laevis embryos. Generally, progression depends on cell type. For example, in Chinese hamster lung cells (Sachs et al., 1974), neuroblastoma cells (Boonstra et al., 1981), and human breast cancer cells (Strobl et al., 1995), membrane potential remains more hyperpolarized compared to spinal cord astrocytes (Macfarlane & Sontheimer, 2000) during S phase (Figure 2.2).

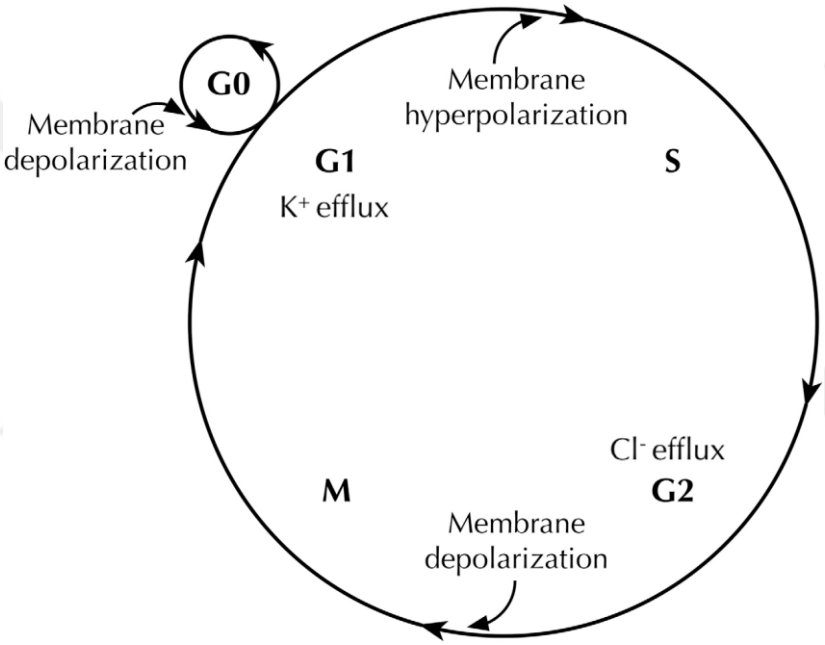

Figure 2.2: Membrane potential changes during cell cycle (Yang & Brackenbury, 2013)

Membrane potential is the difference between intracellular and extracellular potential. It has been shown that the membrane significantly depolarizes in case of tumor progression (Johnstone, 1959; Tokuoka & Morioka, 1957). Also, various *in vivo* and *in vitro* studies proved that the membrane potential of cancer cells is more depolarized than normal cells(Binggeli & Cameron, 1980; Binggeli & Weinstein, 1985; Lymangrover et al., 1975; Marino et al., 1994; Melczer & Kiss, 1957; Redmann et al., 1972; Stevenson et al., 1989; Woodrough et al., 1975) (Figure 2.3).

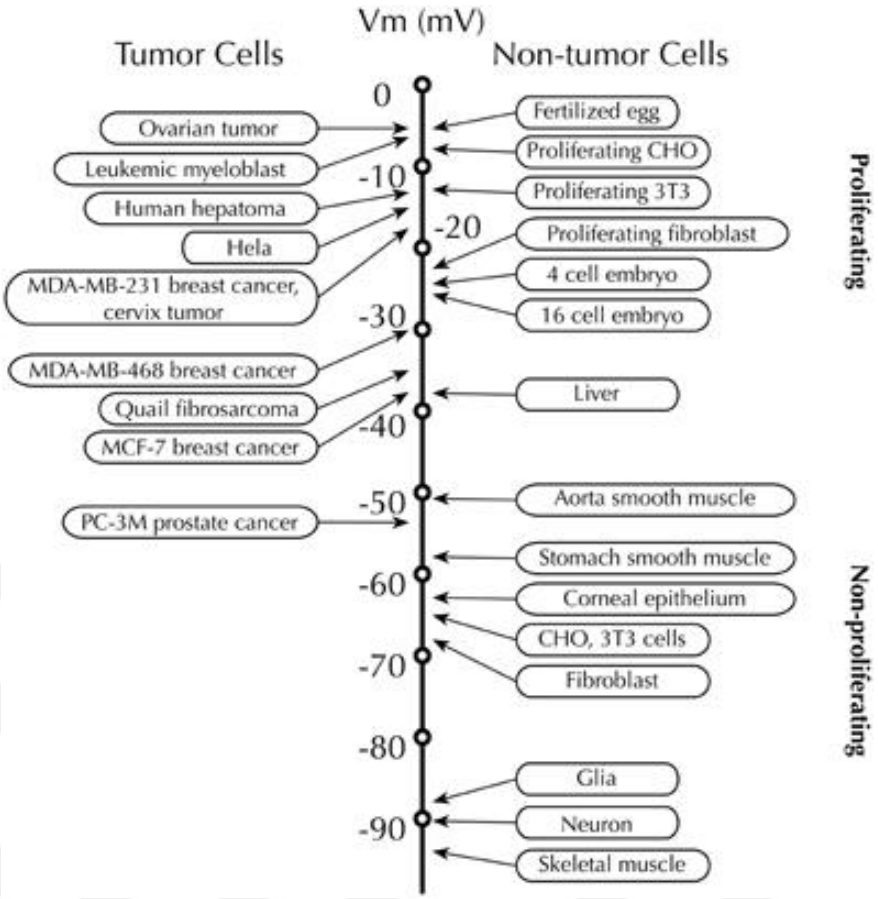

Figure 2.3:Comparison of the membrane potential levels of tumor and nontumor cells (Yang & Brackenbury, 2013)

2.2 The Cell (Plasma) Membrane

A cell membrane is a semi-permeable thin structure (from 7.5 to 10 nm) that defines the boundary of cells by separating them from the extracellular environment (Hine, 2009). The existence of that concept was firstly suggested by Ernest Overton in 1899(Branton & Deamer, 1972). The plasma membrane controls the transition of substances and protects cell integrity.

The plasma membrane is mainly made up of lipid bilayer and proteins (Figure 2.4).

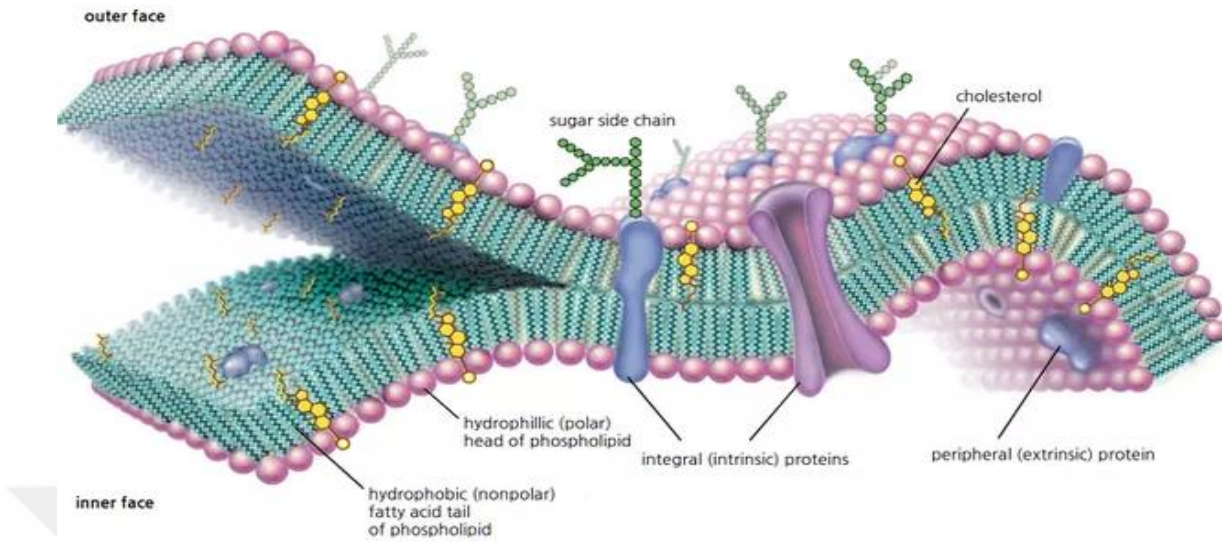

Figure 2.4: Cell membrane structure (Bailey, 2020)

2.2.1 Lipids

In principle, the major part of the membrane consists of phospholipids (Shevchenko & Simons, 2010). Phospholipids are composed of a hydrophilic head and hydrophobic tails. Due to the fact that the inner part of the phospholipid bilayer is hydrophobic, the cell membrane does not allow water-soluble substances to permeate (Cooper et al., 2007). Therefore, phospholipids are excellent candidates for forming cell membranes.

The essential roles of lipids can be listed as energy storage, compartmentalization, and signaling. For instance, signaling lipid phosphatidylserine (PS) behaves as a damage sensor to activate repair proteins by sensing membrane damage in case of injury (Horn & Jaiswal, 2019).

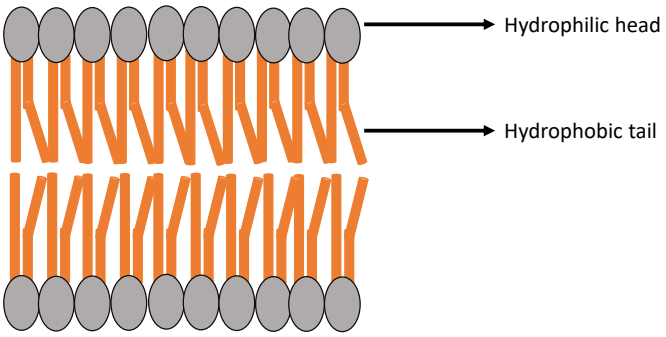

Figure 2.5: Structure of phospholipid molecule

2.2.2 Proteins

Proteins are the second important element of the cell membrane, and each type has its orientation. A membrane may include hundreds of distinct proteins. Plasma proteins may be divided into integral, peripheral, and lipid anchored proteins. Peripheral proteins and lipid anchored proteins exist outside of the lipid bilayer. Transmembrane proteins are the most known type of integral proteins which act as gateways (Loschwitz et al., 2020).

Membrane proteins perform unique functions, including transport, enzymatic activities, signal transduction, and attachment to the extracellular matrix (ECM)(Reece & Campbell, 2011).

2.3 Ion Channels

Ion channels are proteins responsible for ion transition in the cell membrane. They are embedded within the membrane and control ion flow. Depending on energy utilization, ion channels may be either active or passive (Conner & Schmid, 2003). Passive channels are always open, so ion crossing is continuous. However, active channels have a gating mechanism that controls channel opening.

Two distinguishing characteristics of ion channels are ion selectivity and response to external stimuli. More than 100 ion channels have been discovered (Bezanilla, 2008). Based on ion selectivity, ion channels are listed as chloride channels, sodium channels, potassium channels, calcium channels, proton channels, and nonselective channels. On the other hand, they are classified as voltage-gated ion channels, ligand-gated ion channels, light-gated ion channels, temperature-gated ion channels, and nucleotide-gated ion channels by gating (Alberts et al., 2015; Gouaux & MacKinnon, 2005).

2.3.1 Classification by gating

Ligand-gated ion channels

Ligand-gated ion channels, also known as ionotropic receptors (Hucho & Weise, 2001), enable ion flow through the plasma membrane by binding chemical species. The most important type of ligand-gated ion channel is the class activated by the binding of neurotransmitters. Other ligand-gated ion channels are sensitive to chemical signals in the cytoplasm (Dale Purves, 2001). When a ligand is bound to the surface, the channel is

opened. Some examples include nicotinic acetylcholine receptors (nAChRs), adenosine triphosphate (ATP) receptors, γ-aminobutyric acid (GABA), glutamate, glycine, and 5-hydroxytryptamine (5-HT) receptors (Dent, 2010).

Light-gated ion channels

Light-gated ion channels, channelrhodopsins (Josselyn, 2018), are activated in response to light stimuli. Light-gated ion channels may be either natural or synthetically synthesized. In a working manner, light-gated ion channels are not too much different than other gated channels. They are transmembrane protein structures that are opened when exposed to a stimulus. The nicotinic acetylcholine receptor is the first synthetic example of light-gated ion channels (Lester et al., 1980).

Temperature-gated ion channels

Transient receptor potential (TRP) ion channels have temperature-gated detection mechanisms responsible for heat changes. The Transient Receptor Potential Vanilloid (TRPV) subgroup is the most known type. For instance, an increase in temperature up to 42 °C induces channel opening (Reubish et al., 2009). Moreover, among calcium channels, T-type Ca+2 channels are sensitive to both temperature and voltage changes (Iftinca et al., 2006).

Voltage-gated ion channels

Voltage-gated channels are another important family of ion channels that are activated by membrane potential changes. Back in the ’50s, Hodgkin and Huxley discovered voltage-gated sodium currents through studies in squid giant axons (Ruiz & Kraus, 2015).

2.4 Voltage-gated Ion Channels

Voltage-gated ion channels are embedded transmembrane protein complexes activated by variations in cell membrane potential. Those channels are members of a wide gene family and essential for cell activities. Voltage-gated ion channels are mainly responsible for action potential production in excitable cells such as neurons (Isom et al., 1994). Figure 2.6 shows the basic structure of ion channels.

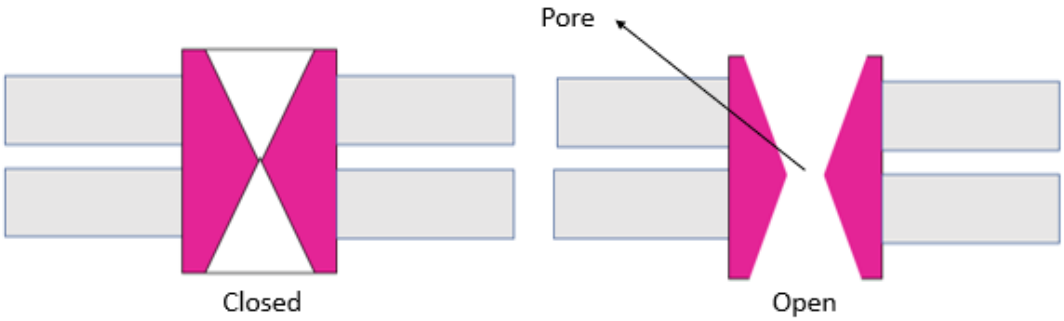

Figure 2.6: Ion selective gated channel structure

According to ion selectivity, the main ion channels are as follows; Na^+, K^+, and Ca^{2+} channels.

2.4.1 Voltage-gated sodium channels

Voltage-gated sodium channels are crucial to initiating action potential, signal propagation, and membrane depolarization (Marban et al., 1998; Wood et al., 2004). They involve a family of nine α subunits (Nav1.1, Nav1.2, Nav1.3, Nav1.4, Nav1.5, Nav1.6, Nav1.7, Nav1.8, and Nav1.9) and each α subunit, which composes of four domains, is in association with auxiliary β subunit (Figure 2.7). Under the resting condition, VGSCs are closed. They are opened when the membrane is depolarized by the influx of sodium ions into the cell and give rise to action potential generation (Yu & Catterall, 2003). There are toxins used in different studies to understand the essential functions of sodium channels such as TTX, STX, and BTX (Denac et al., 2000).

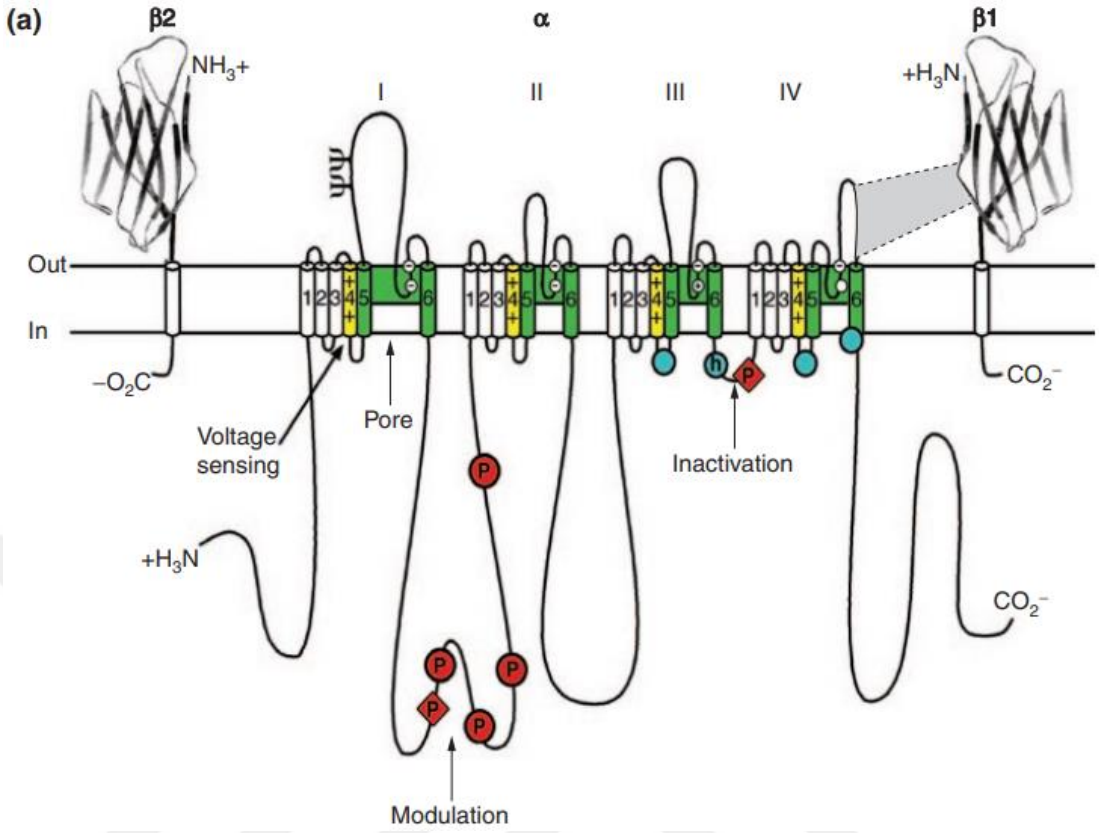

Figure 2.7: Schematic representation of sodium channel subunits (Yu & Catterall, 2003).

2.4.2 Voltage-gated potassium channels

Voltage-gated potassium channels are an important family of ion channels in terms of controlling threshold value for action potential generation and returning the cell to the resting condition, called repolarization (Kang et al., 2000). The efflux of positively charged K^+ ions induce a decrease in voltage in the cell (falling phase). VGKCs including 12 sub-families (K_v1, K_v 2, K_v 3, K_v 4, K_v 5, K_v 6, K_v 7, K_v 8, K_v 9, K_v 10, K_v 11 and K_v 12), are employed for various cellular mechanisms ranging from neuronal excitability to proliferation(Pongs, 1999; Wulff et al., 2009).

2.4.3 Voltage-gated calcium channels

Similar to sodium and potassium channels, VGCCs take an active role in neuronal signals. When the membrane is depolarized, gated channels control and regulate calcium influx (Dolphin, 2006). Moreover, activation of voltage-gated calcium channels triggers various processes, including gene transcription, cell cycle, transmitter release, and

metabolism (Simms & Zamponi, 2014; Zamponi et al., 2015). VGCCs may be categorized into five, including L-type, N-type, P-type, T-type, and R-type.

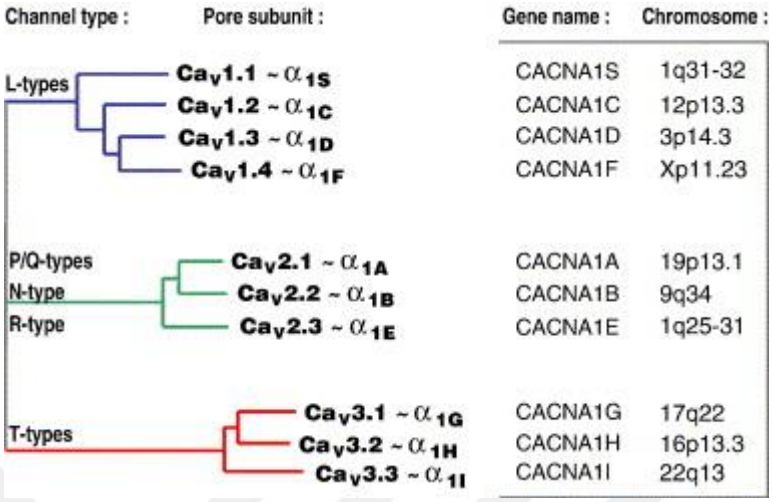

Figure 2.8: Voltage gated calcium channel types and pore subunits (Bidaud et al., 2006)

Recently, Berzingi *et al*. demonstrated the relation between depolarization-activated voltage channels and breast cancer. As explained, sodium, potassium, and calcium take a key role in generating membrane potential. The permeability of ion-selective voltage-gated ion channels gives rise to membrane potential (Yang & Brackenbury, 2013). The relation between permeability and membrane potential is shown by The Goldman-Hodgkin-Katz equation as follows,

$$V_m = \frac{RT}{F} \ln \left(\frac{P_{Na^+} + [Na^+]_o + P_{K^+} + [K^+]_o + P_{Cl^-} + [Cl^-]_o}{P_{Na^+} + [Na^+]_i + P_{K^+} + [K^+]_i + P_{Cl^-} + [Cl^-]_i} \right)$$

Where P is the permeability, V_m is the membrane potential, R is the ideal gas constant, T temperature, and F is the Faraday constant (Goldman, 1943; Hodgkin & Katz, 1949).

2.5 Cell Death

Cell death is a crucial process for maintaining a normal cell cycle. After the development of new cells by the mitotic cycle, excessive cells are removed from the body to keep homeostatic balance constant. The most well-known types of cell death are apoptosis, necrosis, and autophagy.

2.5.1 Apoptosis

Apoptosis, also called programmed cell death, is the process that naturally occurs within the cell to dispose of extra and abnormal cells. It is a mechanism that takes a key

role in development and aging. For example, apoptosis is required for the development of organs and tissues such as fingers and toes.

Apoptosis may occur by either intrinsic (mitochondrial) pathways or extrinsic pathways. Intrinsic apoptosis might happen depending on different cellular signals such as genotoxic damage, ER stress, mitochondrial damage, or the absence of stimulators. In the intrinsic form of apoptosis, negative or positive signals arise based on the released material. For instance, while the lack of cytokines induces negative signals, reactive oxygen species (ROS) or toxic factors cause positive signals (D'Arcy, 2019). Extrinsic pathways are essentially related to death receptors, including Fas receptors, tumor necrosis family (TNF) receptors, and TNP-related apoptosis-including ligand receptors(Xu & Shi, 2007).

The main factors involved in the apoptosis process can be listed as follows:

i. p53
ii. Bcl-2 (B-cell lymphoma 2) proteins
iii. Caspases
iv. Apoptotic protease activating factor-1 (Apaf-1)

p53 gene was discovered by Arnold Levine, David Lane, and William Old in 1979. It is a tumor suppressor protein responsible for deciding whether the cell will be repaired or die during defects (Gupta et al., 2019; Vousden & Lu, 2002). Bcl-2 (B-cell lymphoma 2) proteins family is crucial for intrinsic apoptosis consisting of two opposite groups; proapoptotic and antiapoptotic members. (Singh et al., 2019). Proapoptotic proteins are located in the cytosol and induce apoptosis by increasing cytochrome-c and Apoptosis-inducing factor (AIF). The initiation of apoptosis depends on the activation of caspases, a family of cysteine proteases. Caspases are classified into two as initiator caspases (Caspase 2, Caspase 8, Caspase 9, and Caspase 10) and executioner caspases (Caspase 3, Caspase 6 and Caspase 7)(Wang et al., 2020). Once initiator caspases are activated, they enable the activation of executioners that induces cell shrinkage, protein breakdown, DNA fragmentation, and destruction of the cytoskeleton. Apaf-1 manages apoptosome formation and requires cytochrome-c(Shakeri et al., 2017).

2.5.2 Necrosis

Necrosis is the uncontrolled way of cell death in which the cell loses its integrity and vital functions due to external reasons such as injury, hypoxia, heat, or toxic chemicals. Pathological conditions are mostly associated with necrotic cell death (Proskuryakov et al., 2003). During necrosis, the production of mitochondrial reactive oxygen species increases, and ATP generation decreases.

2.5.3 Autophagy

Autophagy is another type of cell death that aims to get rid of damaged cells to have new ones in the body. It plays an important role in destroying misfolded or aggregated proteins and eliminating intracellular pathogens. Also, it is required for growth and homeostatic balance like apoptosis (Glick et al., 2010; Mathew et al., 2007). Autophagy is ATP dependent process including three phases: initiation, execution, and maturation (Kelekar, 2005).

2.6 Calcium Signaling in Cell Death

Calcium ions are vital in cell signaling. It has been known that those ions are essential for cell survival. However, it has also been shown that an increase in calcium amount causes death. Firstly, Fleckenstein *et al.* estimated the function of Ca^{2+} as a death initiator in cardiomyocytes (Fleckenstein et al., 1974).

Since Ca^{2+} ions are considered as death factors in extreme cases such as overload or perturbation, it has been related that calcium takes a key role in different death modalities (Figure 2.9).

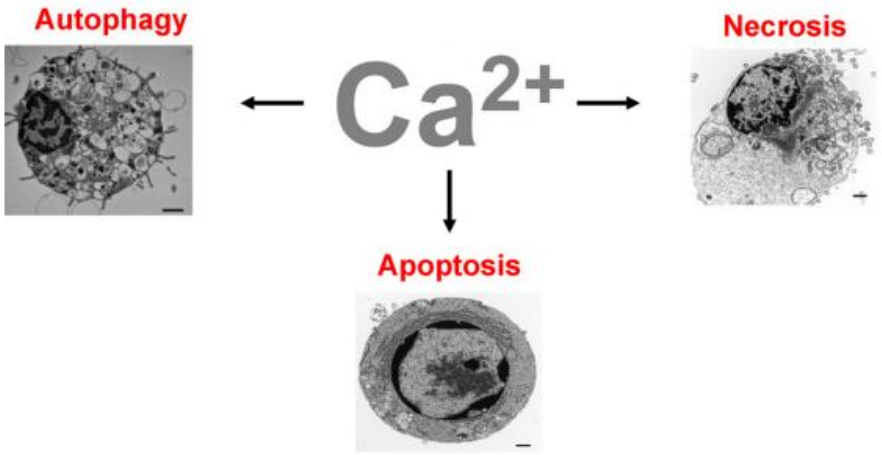

Figure 2.9: Calcium related cell deaths (Zhivotovsky & Orrenius, 2011)

2.6.1 Calcium in apoptosis

Fundamentally, intrinsic apoptotic signaling pathways are associated with mitochondria. Different apoptotic factors are found in the mitochondrial intermembrane space (IMS), including cytochrome c, AIF, and procaspase 9. During apoptotic signals such as DNA damage, oxidative stress, and endoplasmic reticulum (ER) stress, these factors are released into the cytosol, leading to apoptosis. Furthermore, mitochondrial dysfunction modalities such as loss of mitochondrial membrane potential (MMP), increased reactive oxygen species (ROS) production, decreased ATP production, and alteration of mitochondrial Ca^{2+} homeostasis are accepted as the reasons for mitochondria-related apoptosis (Giorgi et al., 2012). Some studies showed that an increase in mitochondrial Ca^{2+} levels may directly damage mitochondrial membrane potential and triggers apoptotic proteins (Csordás et al., 2002; Hajnoczky et al., 2000; Pacher & Hajnoczky, 2001).

In general, Ca^{2+}-driven apoptotic stimulations result in the release of Ca^{2+} from ER and induce the release of apoptotic factors, as explained before.

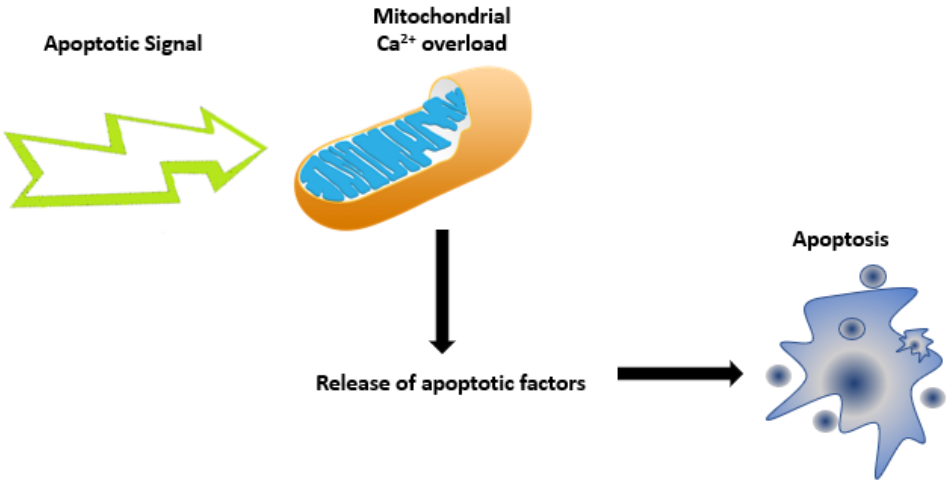

Figure 2.10: Calcium related apoptosis

Another study that Norberg et al. conducted indicated that Ca^{2+}- dependent actions may trigger Apoptosis-inducing factor (AIF) (Norberg et al., 2008). To maintain cellular activities, those calcium ions need to be precisely controlled.

2.6.2 Calcium in necrosis

The necrosis morphologically differs from apoptosis. While apoptosis shapes as cell shrinkage, blebbing or condensed DNA, necrosis is characterized by swelling, breaking of membrane integrity, or lysis. There are many reasons for necrotic cell death, including ischemia and hypoxia, ionic imbalance, mitochondrial variations, and calcium overload. Calcium overload activates proteases such as calpain or serine proteases and induces cell death (Szabo, 2005). During necrosis, the production of ROS increases, and calcium channels are opened.

2.6.3 *Calcium in autophagy*

It is known that autophagy may be induced by ER stress and so correlated with calcium. The first calcium-related autophagy was established in 2007 by Jaattela and colleagues, performing ER calcium stimulation (Hoyer-Hansen et al., 2007).

2.7 Cancer Treatment Methodologies

Although cancer disease is toilsome to treat, there are various approved cancer therapies used in clinics, such as chemotherapy, radiotherapy, targeted therapy, and surgical operation. Surgical removal of the tumor may be the treatment option in cases where cancer is not hematological or metastasized. However, cancer may relapse in the postoperative period. Therefore, chemotherapy or radiotherapy is used when the disease has relapsed, and a surgical approach is not an option. Even though chemotherapy and radiotherapy are very effective therapies, they may cause many side effects and limitations. The most common acute side effects can be summarized as nausea and vomiting, gastrointestinal discomfort, fatigue, anemia, epidermal damage, dry mouth, hair loss, and infertility (Gegechkori et al., 2017).

Besides, chemotherapeutic agents are cytotoxic drugs that block uncontrolled cell division and induce cell death (Malhotra & Perry, 2003; Perazella, 2012). Therefore, targeted treatment methods are being developed to increase the treatment potential of these chemotherapeutic agents and eliminate the negative and inadequate effects of conventional drug therapy. Photodynamic therapy (PDT) and photothermal therapy (PTT) are the most known types of targeted therapies.

The first findings of PDT date back to the 1960s. The working principle of photodynamic therapy is based on the excitation of a photosensitive (PS) agent by light at a specific wavelength. The combination of agent, light, and oxygen causes toxicity and results in cell death (Dougherty et al., 1998). Due to noninvasiveness, selectivity, and fewer side effects compared to drug delivery, PDT plays a big role in cancer treatment. Different irradiation sources such as light emitting diodes (LED) and lasers are used to excite. For effective PDT, penetration of light and PS choice are very crucial. The light should penetrate enough, and PS should have good properties such as biodegradability, circulation time, low manufacturing cost, and stability. Most common photosensitizers are tetrapyrrole structured (Agostinis et al., 2011).

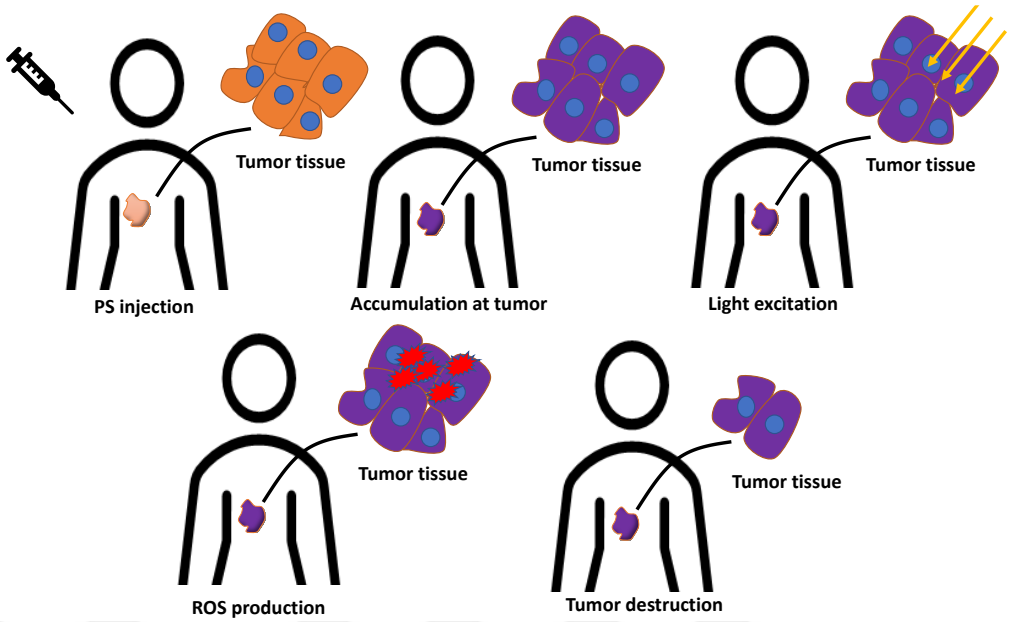

Figure 2.11: Photodynamic therapy

Photothermal therapy is a non-invasive technique that uses electromagnetic radiation, primarily near-infrared radiation, to kill tumor cells. In PTT, light energy is converted to heat energy to cause thermal burns on the tumor. Photosensitizers are employed, like in PDT, to induce damage to cancer tissue. However, tumor tissue is chemically damaged in PDT. Various photothermal agents are employed in photothermal therapy, including nanomaterials and nanocrystals (Zhi et al., 2020). One of the light sources used in PTT is a laser, mainly operating in the near-infrared region (~ 800 nm). When photothermal agents are irradiated by light, heat is produced because of increased kinetic energy by transforming of the agent to an excited singlet state. At 42°C temperature, cell necrosis happens (Li et al., 2020).

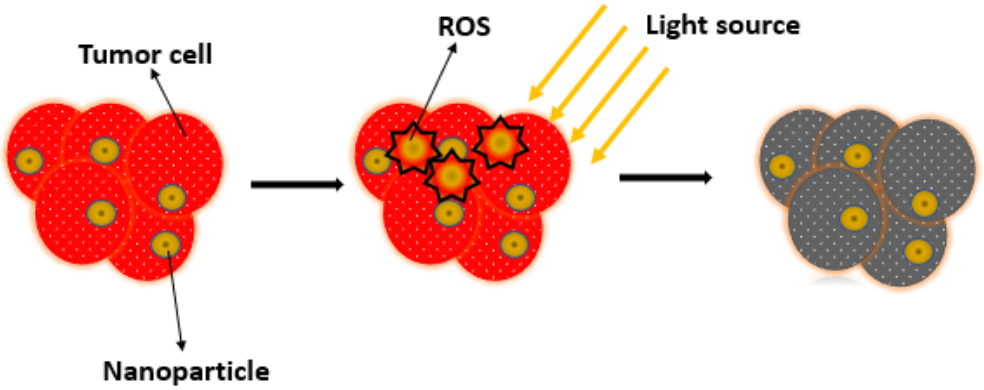

Figure 2.12: Photothermal therapy

2.8 Photoelectrical Stimulation of Cancer Cells

2.8.1 Organic semiconducting polymers for biological tools

Organic polymers are photovoltaic materials that have become significant because of their remarkable features, including high optical absorption coefficients, thermoelectricity, and fabrication techniques (Duda et al., 2013). Those materials convert light to electrical charges (Gunes et al., 2007). Although organic polymers are popular in solar cells, they exhibit functional features in bioelectronic devices from sensing to stimulation. The main idea behind these photoactive interfaces is to take advantage of photovoltaic action in organic material to manipulate bioelectricity. Fundamental examples are organic transistors, microelectrode arrays, and retinal implants (Higgins et al., 2020).

Organic semiconductors act as a bridge between the biological systems (ionic) and the electronic environment. In an illuminated system that consists of semiconductor, photo-induced charges are generated. The movement of charge carriers (e.g., electrons, holes) enables to sense or stimulate cells or tissue by modulating membrane potential. Different types of π- conjugated conducting polymers such as poly (3,4 ethylenedioxythiophene) (PEDOT), poly(3-hexylthiophene2,5-diyl) (P3HT), [6,6]-Phenyl-C61-butyric acid methyl ester (PCBM), have been integrated into those devices (Hsiao et al., 2016) due to their soft and biocompatible nature. In 2011, Ghezzi *et al.* showed for the first time the use of organic semiconductors for photostimulation of neurons. The device is made up of regioregular(rr)-P3HT: PCBM blend deposition by spin coating on Indium-thin oxide (ITO) substrate.

In that bulk heterojunction structure, rr-P3HT is the electron donor while PCBM works as electron acceptor.

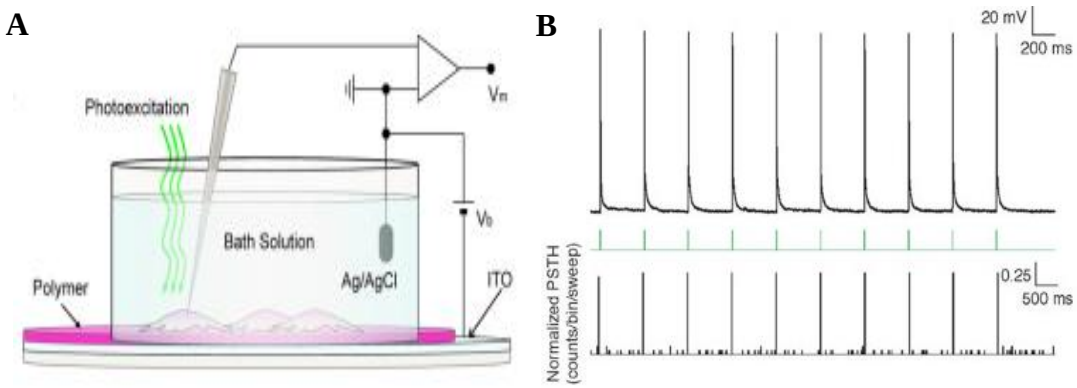

Figure 2.13: A) Schematic of bioorganic interface and patch-clamp set up B) Action potentials generated by 20 ms pulsed light stimulation at 1 Hz. (From (Ghezzi et al., 2011))

In 2014, Benfenati *et al.* performed photostimulation of neocortical astrocytes using the same device structure and determined an important depolarization of membrane potential (Benfenati et al., 2014). Another example of organic polymeric interfaces is the bulk heterojunction of P3HT and poly {[N, N′-bis(2-octyldodecyl)-naphthalene-1,4,5,8-bis(dicarboximide)-2,6-diyl]-alt-5,5′-(2,2′-bithiophene)} N2200, which was used to create neuronal activity in retina (Gautam et al., 2014).

2.9 Conclusion

Since calcium signaling plays a key role in cell proliferation and the cancer cycle, utilizing calcium signaling mechanisms may pave the way for cancer therapies. Another aspect of the cancer cycle is depolarized membranes. Targeting voltage-gated calcium channels to induce cell death by depolarizing membrane potential via photovoltaic technology has been previously shown (Aria, 2021). Therefore, increasing photocurrent levels using different types of organic polymer (electron acceptor) might be effective in decreasing treatment duration. Also, different polymer concentrations and light intensity may enhance photocurrent. We aimed to use two various adherent cell lines to see the general effect.

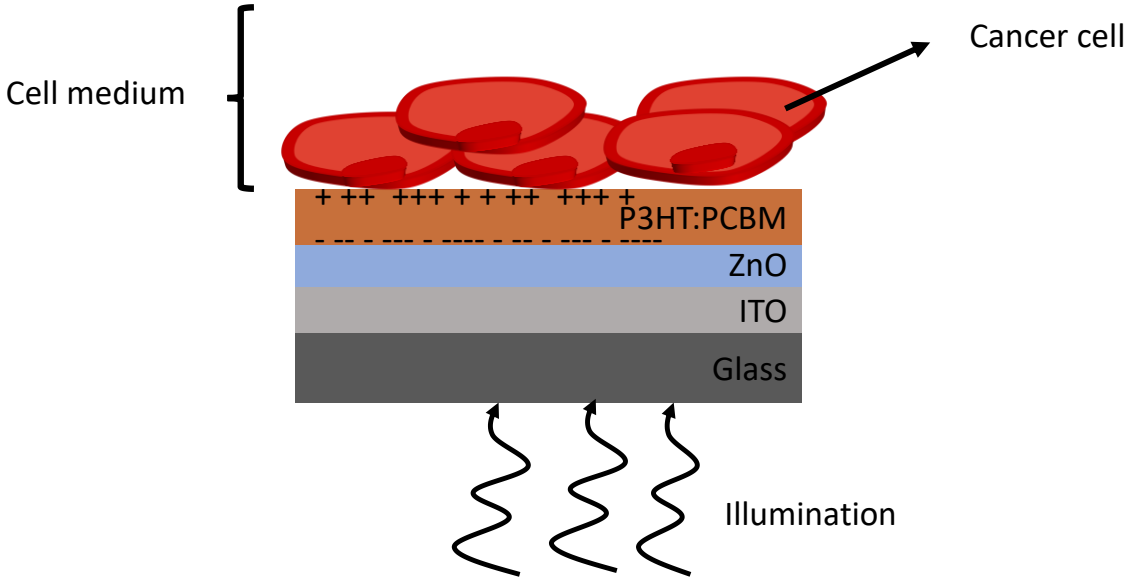

Figure 2.14: Photoelectrical stimulation mechanism

Chapter 3:

MATERIALS AND METHODS

3.1 Cell Culture

MDA-MB-231 (adenocarcinoma, ATCC, HTB-26) and A375-P (melanoma, ATCC, CRL-3224) cell lines were used in the study. The respective culture mediums, catalog numbers, and producing companies are listed in Table 3.1. The cells were cultured in T-75 flasks under 5% CO_2 and 37°C. The base medium was supplemented with 10% FBS and %1 Penicillin Streptomycin. For subculture of MDA-MB-231 and A375-P, cells were washed with sterile PBS and detached from the bottom of flasks with 0.25% Trypsin/EDTA.

Table 0.1 List of materials used in the adherent cell culture

Product name	**Manufacturer**	**Catalog Number**
Dulbecco's Modified Eagle Medium High Glucose	SIGMA	D6429
Fetal Bovine Serum	Thermo Scientific	1050064
Penicillin Streptomycin	PAN-Biotech	P06-07100
Trypsin-EDTA 0.25%	PAN-Biotech	P10-011900
Dulbecco's Phosphate Buffered Saline 1X	PAN-Biotech	P04-36500

3.2 Photoelectrode Fabrication

3.2.1 Cleaning and spin coating

ITO (indium tin oxide) glass substrates (20x15 mm), P3HT (M108, Mw=36,010) and PC70BM (M114, Mw=1031 g/mol) were purchased from Ossila. The sonicator, spin coater (MTI-Spin Coater VTC-100), and heater were used for the substrate fabrication. ITOs were respectively sonicated in distilled water, pure acetone, and isopropanol. The cleaned substrates were dried using a dry air gas cylinder. The ZnO (zinc oxide) solution was prepared by sonicating 219.3 mg zinc acetate dehydrate (Zn (CH3CO2)2·2H2O) in

2 ml of 2-methoxyethanol (C3H8O2) and 80 mg of ethanolamine (HOCH2CH2NH2) (Han et al., 2020) at 50 °C for 20 minutes. Then substrates were annealed at 280 °C for 15 minutes. The photoactive solutions were prepared by using 94.2 % regioregular P3HT (poly(3-hexylthiophene-2,5-diyl)) and >99 % PC70BM ([6,6]-Phenyl-C71-butyric acid methyl ester). 7.5 mg/ml P3HT and 7.5 mg/ml PC70BM was dissolved in 1,2- chlorobenzene and blended (1:1) (Table 3.2).

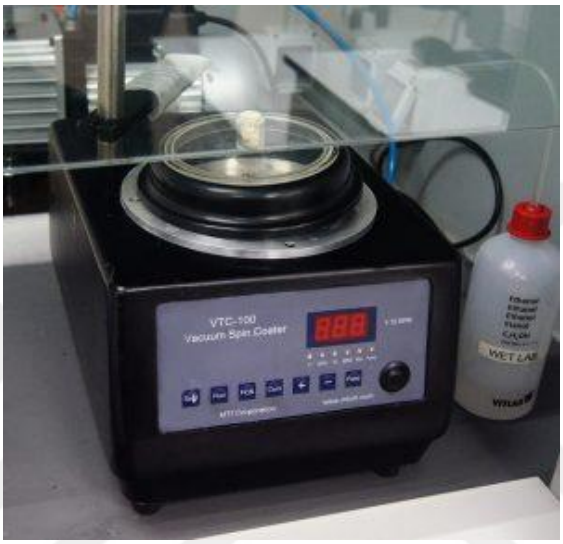

Figure 0.1:MTI-Spin coater VTC-100 used in substrate fabrication

The photoactive solutions were heated at 50°C for 20 min. Photoelectrodes were fabricated by spin coating solution on ITO. Parameters were: 800 rpm and 2 s for the first step and 1500 rpm and 30 s for the second step. Substrates were annealed at 120°C for 2 hours (Ghezzi et al., 2011).

Table 0.2: List of materials and chemicals used in photoelectrode fabrication

Product name	**Manufacturer**	**Catalog Number**
Indium Thin Oxide Glass Substrates Unpatterned 15x20 mm	Ossila	S111
P3HT (Mw=36,010)	Ossila	M108
PC70BM	Ossila	M114
Toluene ≥99.5%	Isolab	973.015
Zinc Acetate Dihydrate	Merck	1088020250
1,2-Dichlorobenzene	Merck	8032382500
Ethanolamine	Sigma	411000

2-Methoxyethanol	Sigma	284467

3.3 Light Set Up and Treatment

Blue power LEDs were used for the photostimulation of cells. In light set up, 2-channel PWM generator was used to control light frequency. Thorlabs PM100D Power meter S121C was used to measure the power.

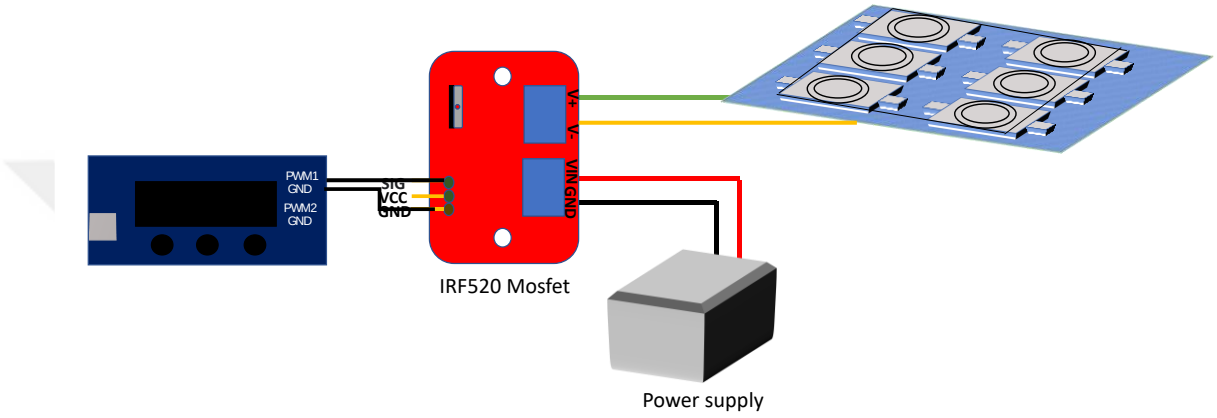

Figure 0.2:Light set up

3.3.1 Photoelectrical stimulation of cells

ITOs were placed into 6-well plates, and cells were cultured on substrates. The light pulses of 3 Hz square wave light stimulations were used over 1.5 hours of light treatment. Substrates were illuminated from the backside by LEDs.

3.4 Test of Cell Viability

Trypan blue exclusion method was used for viable cell counting. In trypan blue counting, dead cells take up dye which live cells do not. Therefore, staining enables the discrimination of cells.

Suspended cells were diluted 1:1(100 µL of cells: 100 µL of trypan blue) by 0.4% trypan blue (Thermo Fisher Scientific, HY-SV30084.01) and incubated in a hood for 5 minutes. After incubation, 10 µL of the mixture was applied to the hemocytometer to fill chambers. Then hemocytometer was placed under the microscope and focused on cells. Stained and unstained cells were counted separately. All cells in four ‘1x1’ mm^2 squares

were counted and averaged to find the total cell number per ml. Then, the number was multiplied by dilution factor (2) and 10^4.

Cell viability was calculated as follows:

$$Viable\ cells\ \% = \frac{(total\ number\ of\ viable\ cells)}{(total\ number\ of\ cells\ )} * 100$$

Three biological and three technical replicates were studied (n=3).

3.5 Flow Cytometry

The manufacturer's protocol (BioLegend FITC Annexin V Apoptosis Detection Kit with PI, 640914) was used to perform flow cytometry. Briefly, trypsinized cells were suspended in Binding Buffer with a final concentration of $1*10^6$ cells/ml. Then FITC Annexin V and PI were added, and cells were incubated for 15 minutes at room temperature in the dark. After that, samples were analyzed using CytoFlex, Beckman Coulter flow cytometry device. 10000 events were recorded for each experimental group.

Table 0.3: FITC Annexin V apoptosis detection kit with PI components

Product name	**Manufacturer**	**Catalog Number**
FITC Annexin V 0.5 ml	BioLegend	640914
Propidium Iodide Solution	BioLegend	640914
Annexin V Binding Buffer	BioLegend	640914

Table 0.4: Excitation and emission parameters of Annexin V and PI

	Excitation(nm)	**Emission(nm)**
Annexin V	488	525
Propidium Iodide	633	660

3.6 Hoechst Staining and Calcium Imaging

Initially, 50 µg of lyophilized Fluo-4 AM was dissolved in DMSO to a final concentration of 1µM. After light treatment, Fluo 4 AM (1:5000), and Hoechst 33342 (1:10000) stains were added and incubated for 20 minutes. Samples were analyzed in a

fresh medium. The images of the Brightfield, Hoechst 33342 (H33342, cell nucleus indicator), and Fluo-4 AM (F4AM, calcium indicator) were taken for each group using Zeiss Live Cell Imaging System. Imaging parameters were:

Brightfield: 0.45 ms exposure time

H33342: 461 nm emission, 150 ms exposure time

F4AM:509 nm emission, 50 ms exposure time

Calcium fluorescence intensities were analyzed using ImageJ, which is open-source software. Fluorescence was calculated by selecting six cells and six backgrounds equal to cell sizes from each image.

The following formula was used for calculations:

$$Corrected\ total\ cell\ fluorescence = Integrated\ Density - (Area\ of\ selected\ cell * Mean\ fluorescence\ of\ background\ readings)$$

3.7 ROS Analysis

Muse Oxidative Stress Kit (Luminex) was used to quantify oxidative stress in our four groups. Muse kit includes the dihydroethidium (DHE) reagent that has been commonly used for the ROS detection in both adherent and suspension cells. DHE reagent works based on the fluorescence detection of superoxide and hydrogen peroxide. When DHE reacts with superoxide ions, oxidation results in red fluorescence (Owusu-Ansah et al., 2008). Two different populations are distinguished in the assay, including ROS (-) and ROS (+) cells. The cell pellet was suspended to 1x10^6/ml with 1X Assay Buffer. An intermediate solution was prepared by diluting Muse Oxidative Stress Reagent to 1:100 with 1X Assay Buffer. Then, the oxidative stress working solution was prepared by diluting the intermediate solution to 1:80 with 1X Assay Buffer. 50 µl of cell suspension and 150 µl of working solution were mixed and incubated at 37°C for 30 minutes. Guava Muse Cell Analyzer was run to perform measurements.

Table 0.5: Muse oxidative stress kit components

Product name	**Manufacturer**	**Catalog Number**
Muse Oxidative Stress Reagent	Luminex	4700-1665
1X Assay Buffer	Luminex	4700-1330

Chapter 4:
RESULTS

4.1 Photocurrent Measurements and Optimization

The photocurrent response of the surfaces was investigated in the DMEM medium. VSP-300 Potentiostat, Biologic, Chronoamperometry was used to measure photocurrent, and photoelectrodes were pumped under the illumination of blue power LEDs. Three-electrode configuration was used for recordings. In the three-electrode scheme, the current flows between the working electrode (WE) and counter electrode (CE). In our case, the working electrode was the device we wanted to measure (ITO/ZnO/P3HT: PCBM), and platinum was used as the counter electrode. The third electrode, Ag/AgCl, was the reference electrode (RE), whose potential was stable.

Different polymer concentrations, light intensities, and frequencies were tested using blue LEDs. We have obtained maximized photocurrent level mixing 7.5 mg/ml P3HT and 7.5 mg/ml PC70BM with a blending ratio of 1:1, compared to 12 mg/ml P3HT and 20mg/ml PC70BM polymer concentration (Figure 4.2D). The optimized photocurrent value, 400 µA, was recorded with 150 mW/cm^2 light intensity and 10 ms pulse duration at 3 Hz (Figure 4.1). To investigate the temperature variations at the polymer/medium interface, we recorded the temperature values over 4 hours of light treatment in the incubator. While the incubator temperature was always constant at 37 °C, the temperature increased from 37°C to 37.9°C at the interface (Appendix B.0.2).

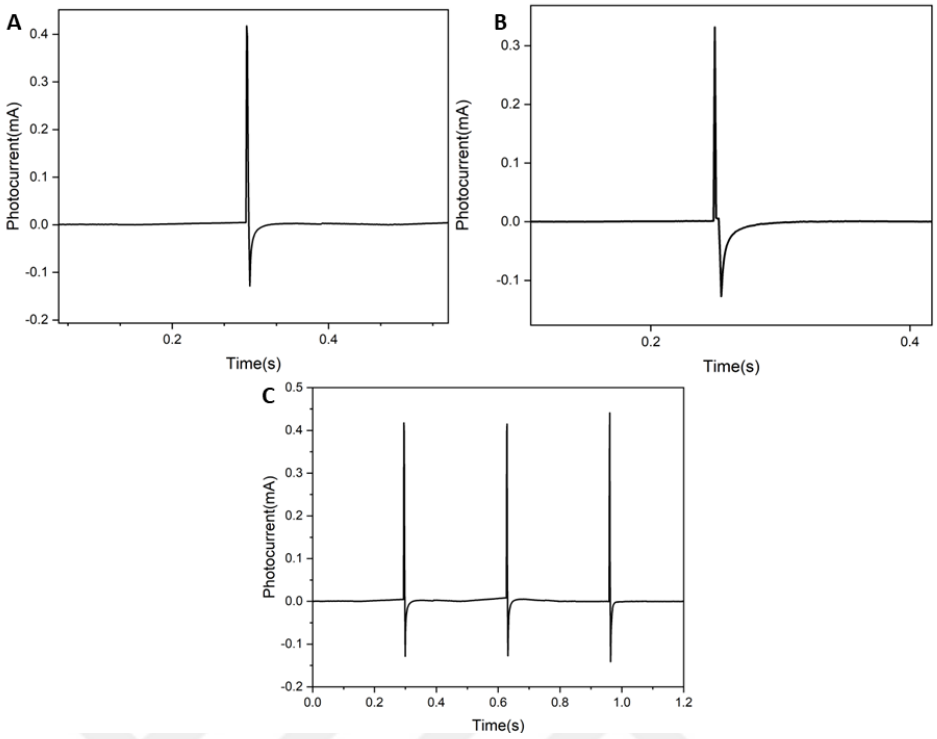

Figure 4.1:Photocurrent level of ITO/ZnO/P3HT:PCBM photoelectrode under the illumination of A)10 ms pulse B)100 ms pulse at 3 Hz with 150 mW/cm^2 light intensity C) 10 ms pulse train

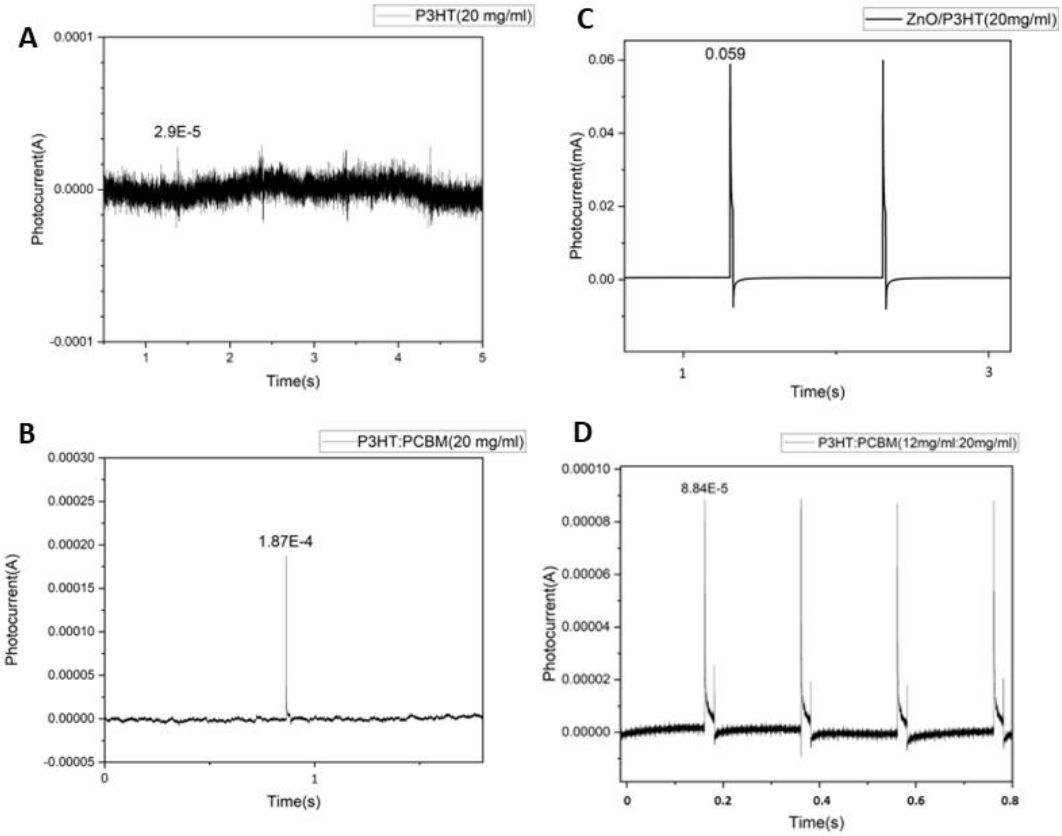

Figure 4.2: Photocurrent levels of different substrates from A to D: ITO/P3HT with 12 mW/cm^2 light intensity at 1 Hz, ITO/P3HT:PCBM with 15mW/cm^2 intensity at 1 Hz, ITO/ZnO/P3HT with 180 mW/cm^2 intensity, 12 mg/ml P3HT and 20 mg/ml PCBM.

4.2 Extracellular Matrix Optimization (ECM)

The proper extracellular matrix is critical to protect cell morphology eliminating undesirable effects of polymer. There are various types of natural substances used as ECM, including polylysine (PLL), poly-D-lysine (PDL), fibronectin, and matrigel (Kleinman et al., 1987; Mazia et al., 1975). The MDA-MB-231 cells that were directly cultured on polymer-coated surfaces without ECM could not grow in natural morphology (Figure 4.3A). Therefore, 0.5 mg/ml PLL, 0.5mg/ml gelatin and fetal bovine serum (FBS) were tested. As seen in Figure 4.3B, cell attachment was not successful in the PLL case. We got the most confluency with the FBS coating of substrates.

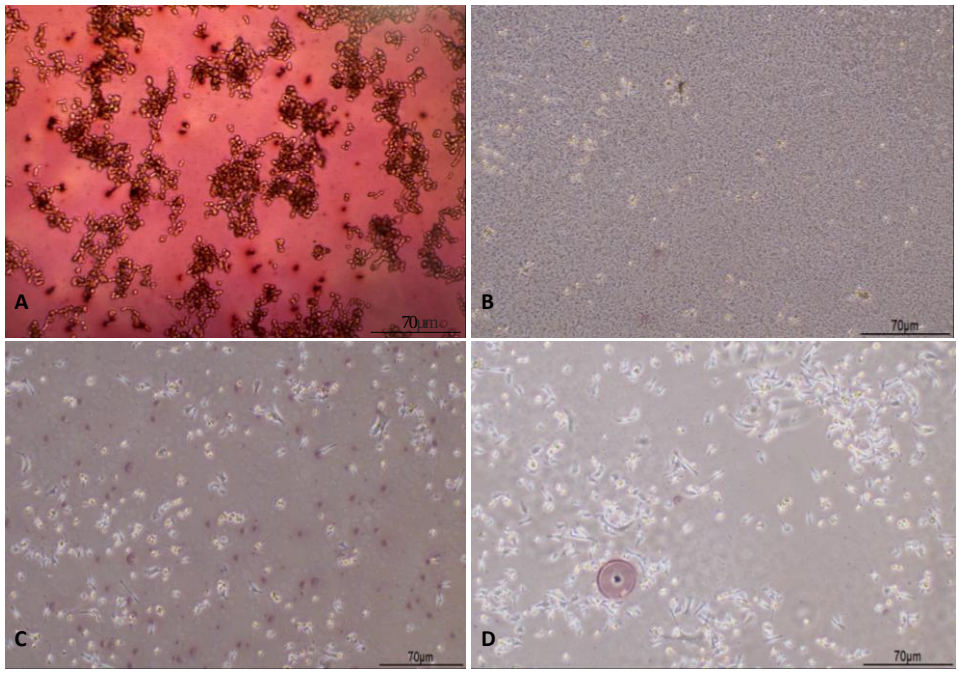

Figure 4.3:Cells grown on top of A)20 mg/ml P3HT:PCBM coated ITO without any ECM coating B) 7.5 mg/ml P3HT:PCBM coated ITO with 0.5 mg/ml PLL coating C) 7.5 mg/ml P3HT:PCBM coated ITO with 0.5 mg/ml gelatin coating D) 7.5 mg/ml P3HT:PCBM coated ITO with FBS coating

4.3 Treatment Duration

Initially, we started to treat cells overnight, and we observed that although overnight treatment is effective, duration might be long and disadvantageous. Therefore, we started to decrease it periodically by increasing the photocurrent level. Cell morphology was similar at the end of the first 30 minutes (30′) in all groups (Figure 4.4A, D, G, K). After 90 minutes of treatment, we observed apoptotic morphology, particularly in the treated coated group (Figure 4.4C and I). Then, the shortest treatment time was set to 90 minutes

(90′) with the current photocurrent that we obtained from the device. Ninety minutes of light treatment with blue LEDs led cells to death in both cell lines.

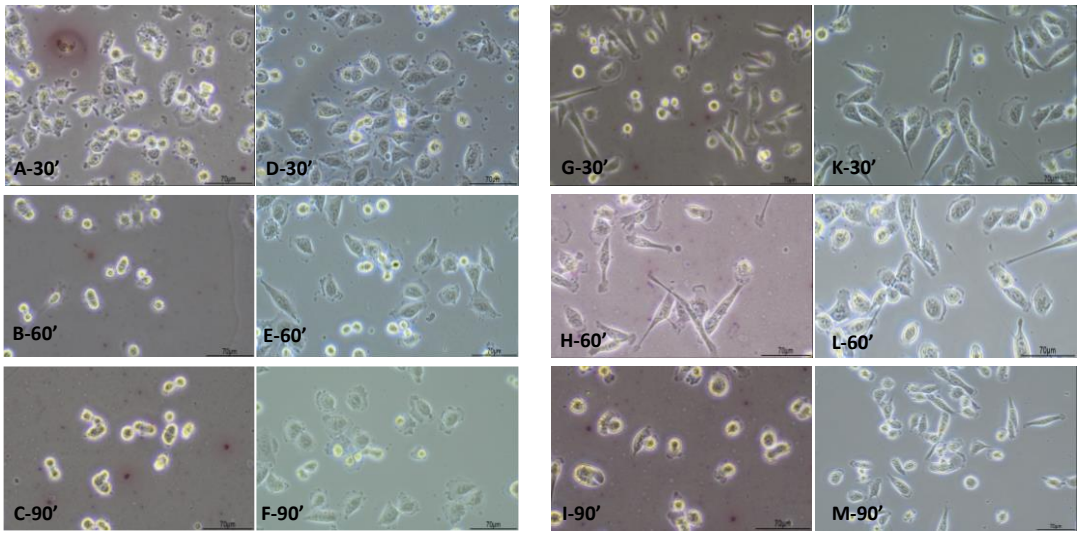

Figure 4.4: Microscope images of A375-P cells over 30 minutes (30'), 60 minutes (60') and 90 minutes (90') treatment, respectively A, B, C represent polymer coated group and D, E, F show noncoated group. Microscope images of MDA-MB-231 cells over 30 minutes (30'), 60 minutes (60') and 90 minutes (90') treatment, respectively, G, H, I represent polymer coated group and, K, L, M show noncoated group.

4.4 Cell Viability

Four different groups were tested to analyze cell viability: a) nontreated noncoated group (control group, NTNC), b) nontreated coated group (NTC), c) treated noncoated group (TNC), and d) treated coated (TC) group. Nontreated noncoated group represents the control group, so cells were directly grown on ITO. Nontreated coated group was used to show the coating effect in cell death. Treated noncoated group indicates the blue light effect in cell death. Finally, treated coated group is the group in which we demonstrate the photocurrent effect (Figure 4.5).

Cell viability was tested by the trypan blue counting method. Among four groups, cell viability has decreased at least 50% in the treated coated group in both cell lines. Also, blue light caused a 17% decrease in MDA-MB-231 cells and a 34% decrease in A375-P cells (Figure 4.6).

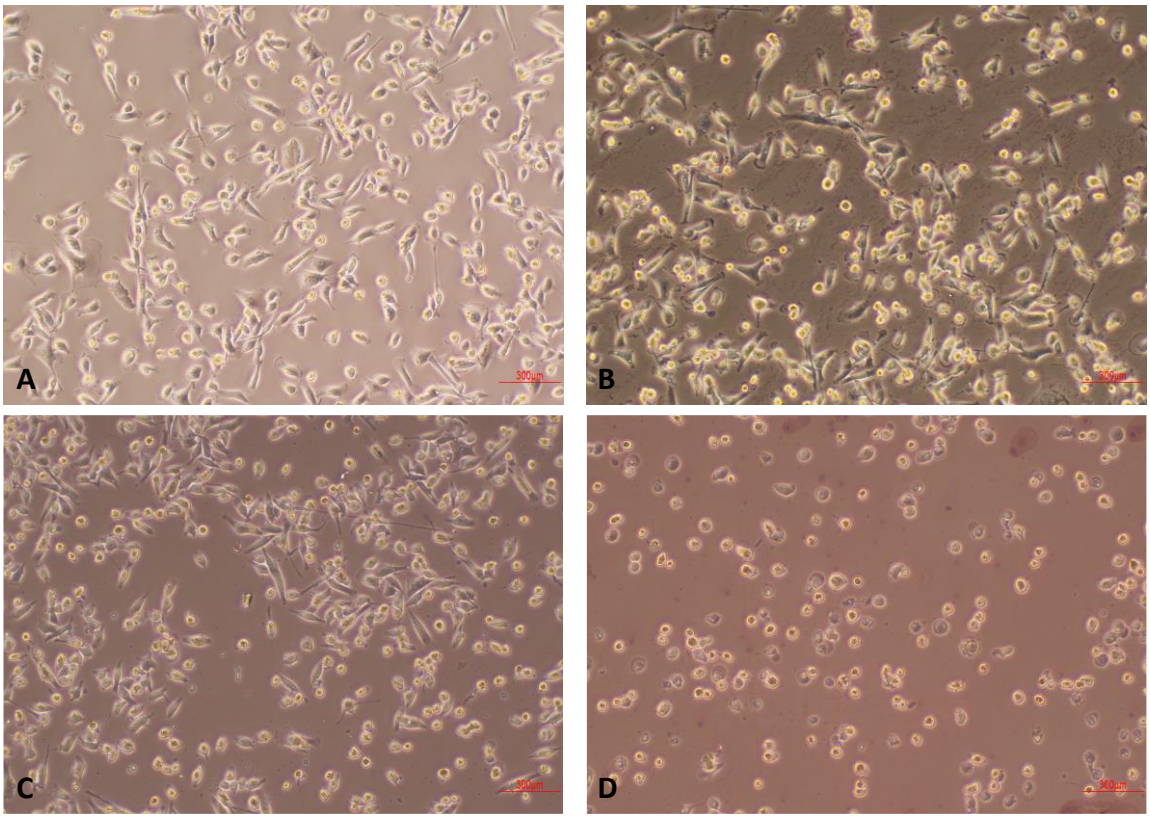

Figure 4.5:MDA-MB-231 cells A) Nontreated noncoated (NTNC) group B) Nontreated coated (NTC) group C) Treated noncoated (TNC) group D) Treated coated (TC) group

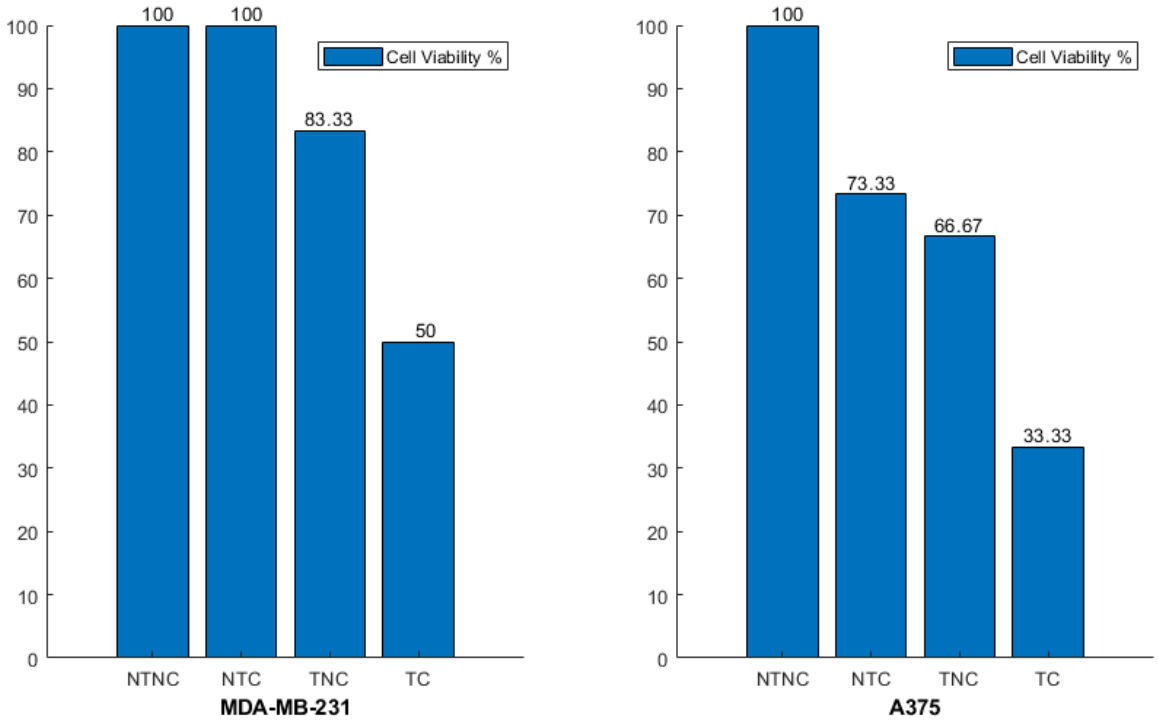

Figure 4.6:Trypan blue counting results of MDA-MB-231 cells(A), A375-P cells (B).

4.5 Flow Cytometry

Flow cytometry was used to detect and quantify apoptosis/necrosis in experiment groups. Each quadrant seen in the graph represents different stages of cell death. In detail, Annexin V +/PI+ part shows late apoptosis while Annexin V +/PI – demonstrates early apoptosis. The first quadrant (LL) means Annexin V-/PI-, which gives information about the viable cell population (Figure 4.7A). Figure 4.7A shows that 93.6% of cells were initially viable cells. However, 1.67% were PI positive, and 4.66% were dead cells. After the 1.5 hours of light treatment, cell viability decreased to 87.86% in the noncoated treated group and 81.88% in the treated coated group. On the other hand, the late apoptotic population has increased almost two times (9.85%) in the noncoated treated group and three times (15.05%) in the treated coated group. (Figure 4.7D).

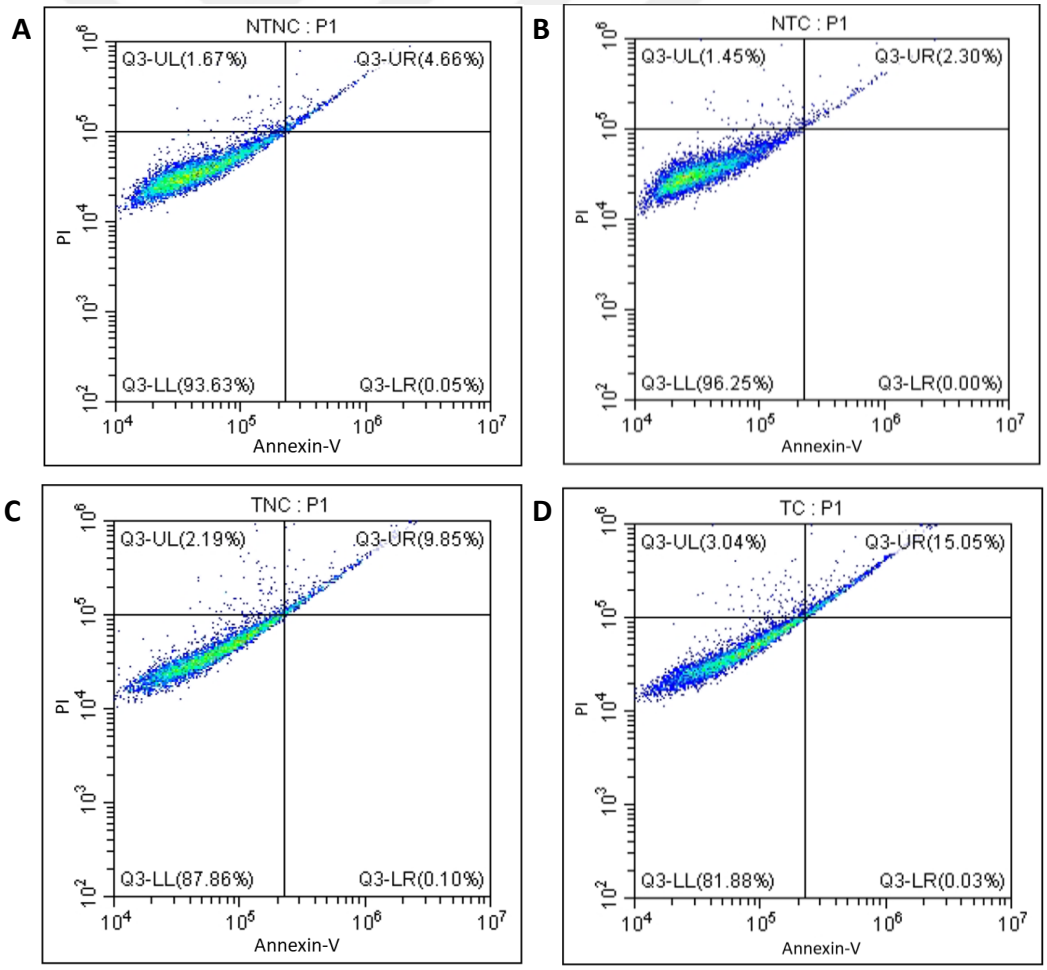

Figure 4.7 Annexin V and PI staining results of A375-P cells A) Nontreated noncoated group B) Nontreated coated group C) Treated noncoated group D) Treated coated group

4.6 Hoechst and PI Staining

Hoechst and PI Live Cell Imaging was performed to identify apoptotic cells. While Hoechst 33342 dye served to stain the DNA of cells, PI was used to distinguish dead cells in the experimental groups. To explain, highly condensed or fragmented bright blue chromatin indicates viable cells with an apoptotic nucleus. Pink chromatin, which shows an organized structure, shows dead cells with normal nuclei. Highly condensed or fragmented bright pink chromatin indicates dead cells with apoptotic nuclei. As seen in Figure 4.9 and Figure 4.10, nontreated groups did not give any signals. However, images showed that the death cell population increased in the treated coated group compared to others.

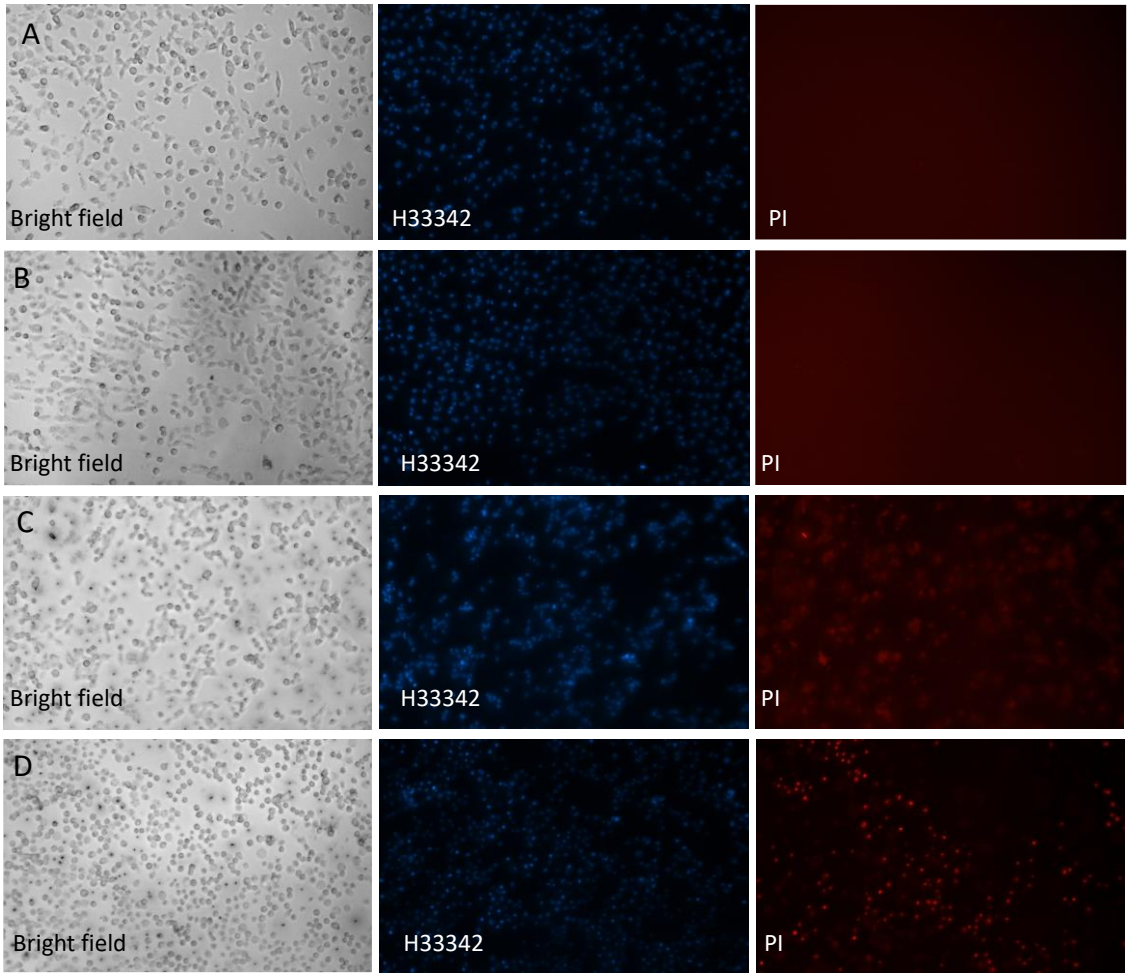

Figure 4.8: Bright field, Hoechst, and PI staining images of A375-P cells A) Noncoated nontreated group B) Noncoated treated group C) Nontreated coated group and D)Treated coated group

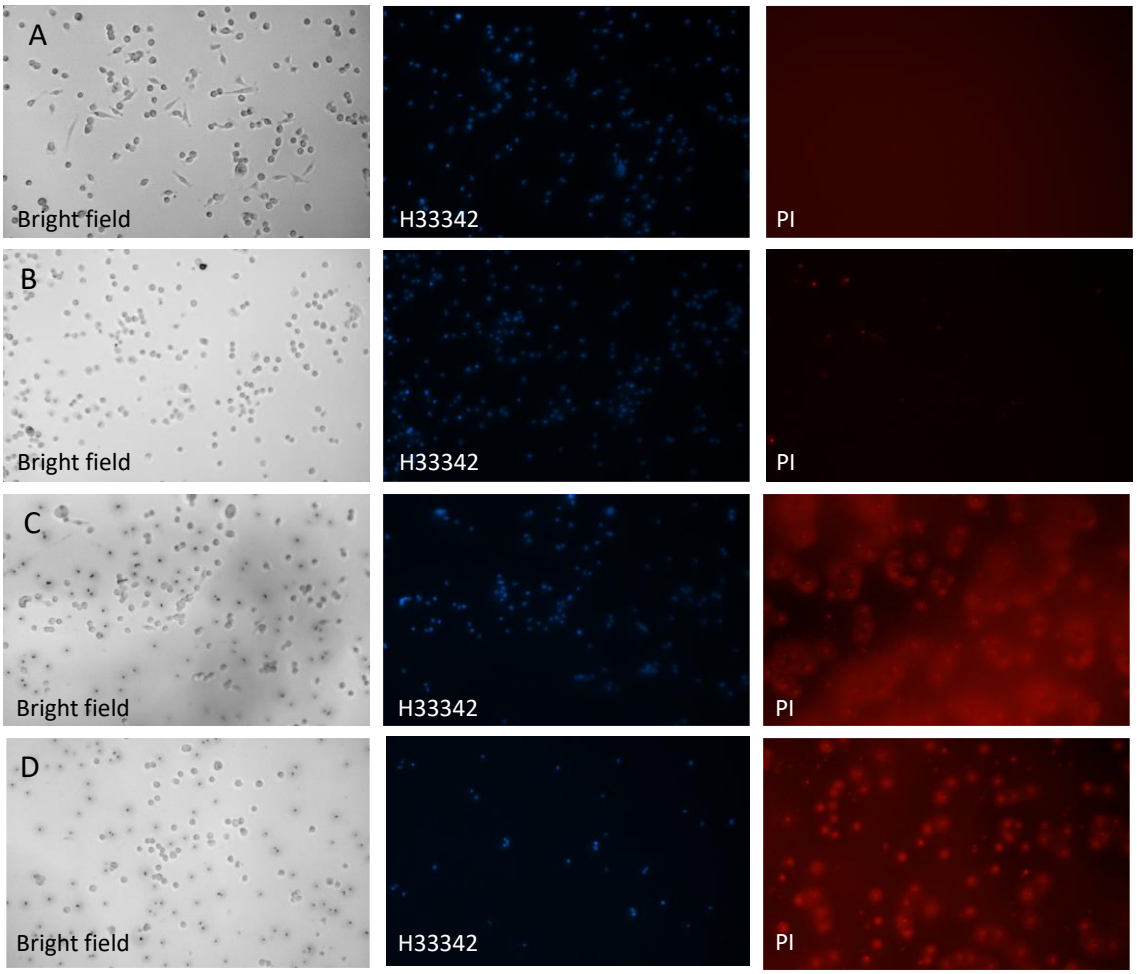

Figure 4.9: Bright field, Hoechst, and PI staining images of MDA-MB-231 cells A) Noncoated nontreated group B) Noncoated treated group C) Nontreated coated group and D) Treated coated group

4.7 Calcium Imaging and ImageJ Analysis

Fluo4-AM was used as a fluorescent Ca^{2+} indicator to monitor calcium activity in four groups. After the Live Cell Imaging, images were analyzed using ImageJ. The highest fluorescence intensity was calculated in the treated coated group, which means more calcium signals were detected (Figure 4.11 and Appendix B.0.3). ImageJ analysis demonstrated that intracellular calcium levels have increased from 1 (AU) to 45(AU) in A375-P cells (Figure 4.12) and 25 (AU) in MDA-MB-231 cells (Appendix B.0.3).

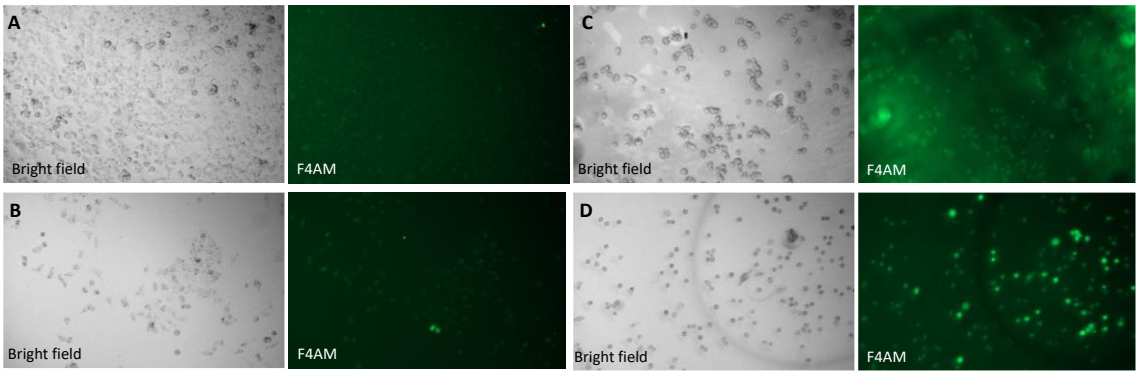

Figure 4.10: Fluo4 AM imaging results of A375-P cells A) Nontreated noncoated group B) Noncoated treated group C) Nontreated coated group D) Treated coated group

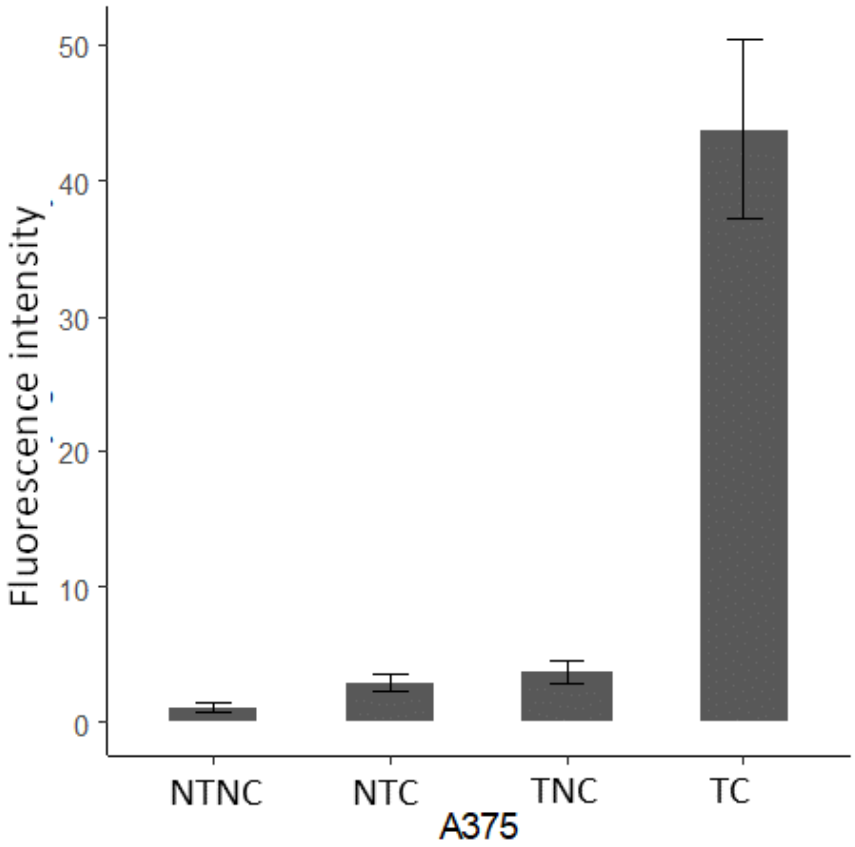

Figure 4.11: Fluorescence intensity graph of A375-P cells

4.8 ROS Measurements

We investigated the ROS production level in all groups to see the alterations in the presence of photocurrent. Our data represented in Figure 4.13 and Appendix B.0.1 indicates ROS measurements. Two events were visualized, including M1 and M2. Briefly, M1 indicates ROS negative cells, and M2 shows cells with ROS activity. The relative percentages of M1 and M2 events were not significantly different in NTNC (M1=95.23%, M2=4.70), NTC (M1=95.37%, M2=4.53), and NCT (M1=94.4%, M2=5.40%) groups of A375-P cells. Furthermore, ROS positive profile, M2, increased approximately two times more (9.90%) in the treated coated group (Figure 4.13). In the second cell line, MDA-MB-231, treated cells grown on coated surfaces showed 19.97% ROS activity (Appendix B.0.3). That can be explained by redox reactions. One of the main photostimulation mechanisms occurring at the polymer/living system interface is reduction/oxidation (redox) reactions, including ROS production (Negri et al., 2020). Photostimulation induces mitochondrial membrane potential depolarization and enhances Adenosine Triphosphate (ATP) and ROS production. Previously, studies indicated that produced ROS due to the redox reactions is at a non-toxic level (Antognazza et al., 2019; Di Maria et al., 2018; Lodola et al., 2017).

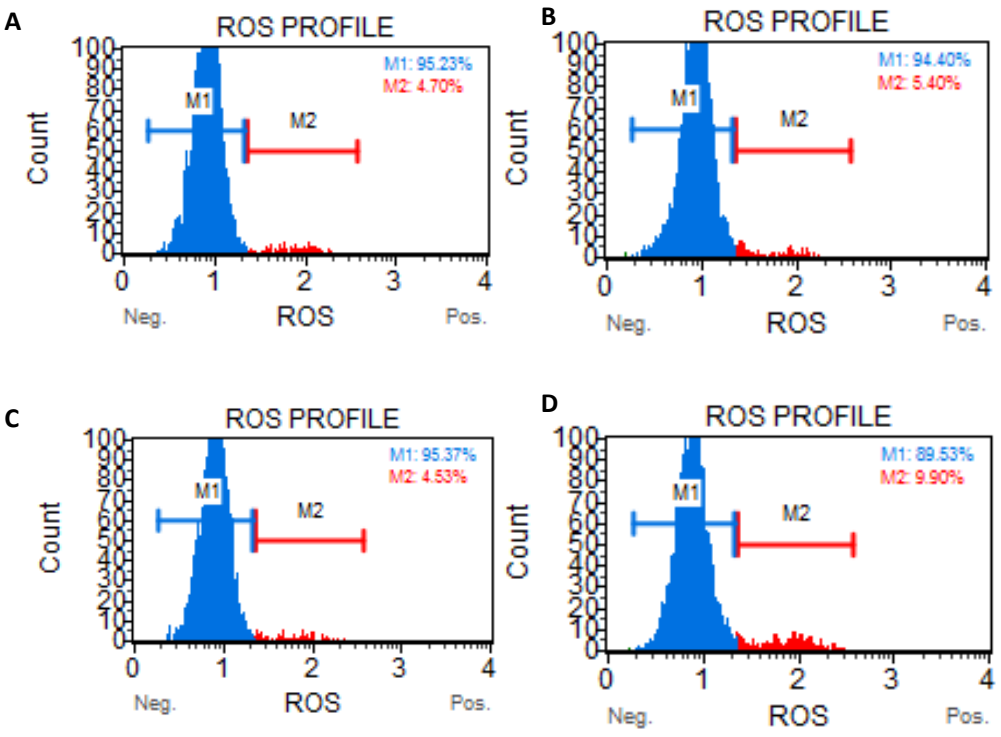

Figure 4.12: Muse Kit ROS measurement results of A375-P cells A) Nontreated noncoated group B) Nontreated coated group C) Treated noncoated group and D) Treated coated group

Chapter 5:
CONCLUSION AND PERSPECTIVES

In this work, we indicated that using a hybrid interface might decrease photoelectrical stimulation duration, leading cancer cells to apoptosis or necrosis. Herein, we characterized different parameters, including light intensity, frequency, and polymer concentration, to get an optimized photocurrent level. We employed light intensities from 12 mW/ cm2 up to 150 mW/cm2 to have the lowest cell viability at the end of treatment. The most efficient polymer concentration was obviously 7.5 mg/ml with a blending ratio of 1:1.

We observed that fetal bovine serum was the most suitable ECM to provide the structural framework in both cell lines among the ECM structures used in the experiments. We think that not only fibronectin but also the bovine equivalent of vitronectin in serum might help to adapt cell attachment to the polymer-coated semi-conductive site; yet further observations are needed (Hayman et al., 1985). The current photocurrent level obtained from the device helped to decrease treatment duration from 24 hours to 1.5 hours. We presented an accurate result showing that increased photocurrent level might decrease treatment time to induce cell death. Therefore, this MSc thesis may give rise to the characterization of new devices to lower cell viability by generating a higher photocurrent.

Cell viability analysis demonstrated that photoelectrical stimulation of cancer cells through alteration membrane potential decreases viability. However, FBS coating was less effective in A375-P cells than in MDA-MB-231 cells. In this regard, other coating materials can be an option, as mentioned in chapter 4.2. Hoechst and PI staining images showed a positive agreement with cell viability results. Flow cytometry quantified the viable and dead cell populations, including necrosis and early/late apoptosis.

Apart from all these, intracellular calcium signal fluctuations due to photoelectrical stimulation were tested. Intracellular calcium signal imaging was performed by Fluo4 AM loading. Fluorescence intensity came out to be the highest in the photostimulated group.

For the ROS effects produced through treatment duration, toxicity measurements were performed. Based on the data, ROS positive profile was higher in the treated coated group than in others. That can be explained by the redox reactions that occurred at the

device/cell interface (Bossio et al., 2018; Tullii et al., 2017). Cancer cells have a more depolarized membrane than healthy cells, as mentioned in Chapter 2.1. So, we think it would be harder to depolarize the membranes of healthy cells than cancer cells (Berzingi et al., 2016). In that case, ROS production levels of healthy cells around the tumor microenvironment would be less than expected. Therefore, healthy human breast epithelial cells may be tested in the first step of future studies.

Babu et al. (2017) recently performed a PDT to induce mitochondria-mediated apoptosis using squaraine in MDA-MB-231 cells. Compared to accumulated ROS levels revealed in that work, our results are considerably lower, which might be improved and controlled for future perspectives. Besides, the temperature change was recorded on top of the polymer/electrolyte interface along 4 hours of light treatment and observed no significant temperature increase compared to PTT levels (Figure B.0.2).

Appendix A: Scanning Electron Microscopy (SEM) and EDX Analysis

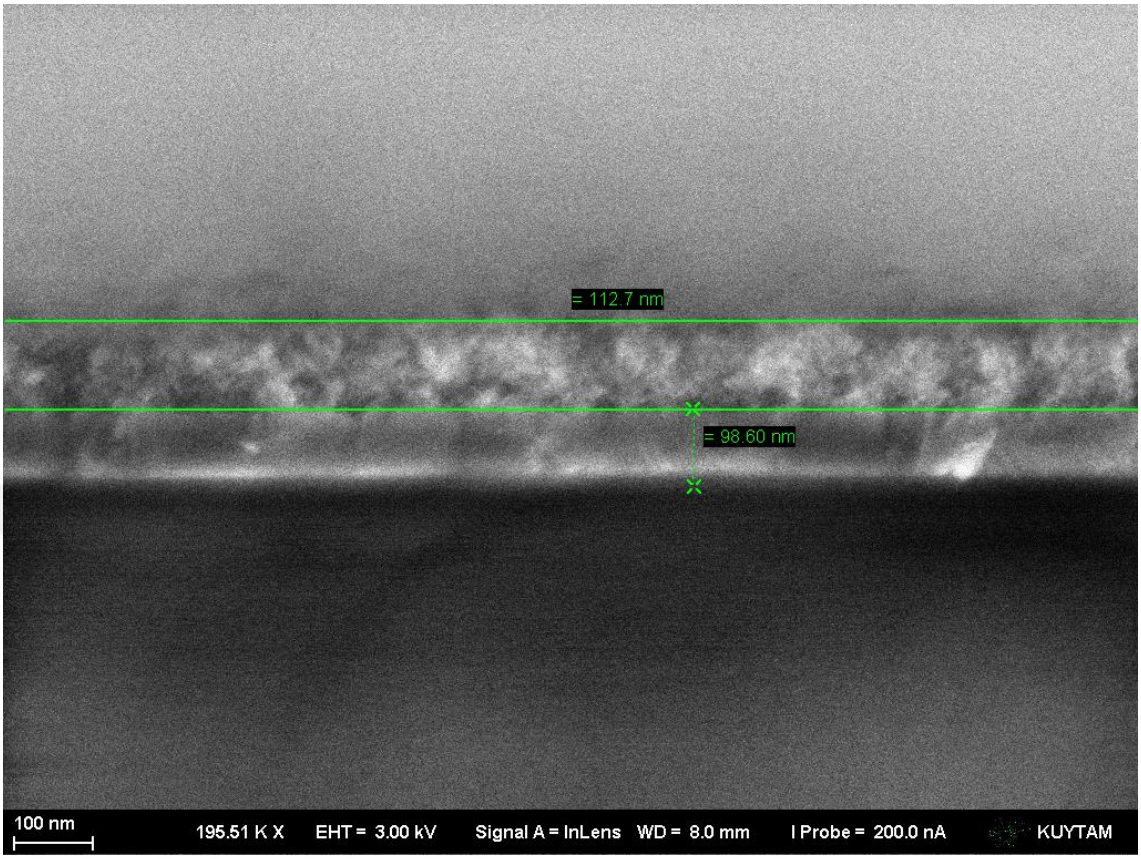

Figure A.0.1: SEM Image of Glass/ ITO/ZnO/P3HT:PCBM photoelectrode

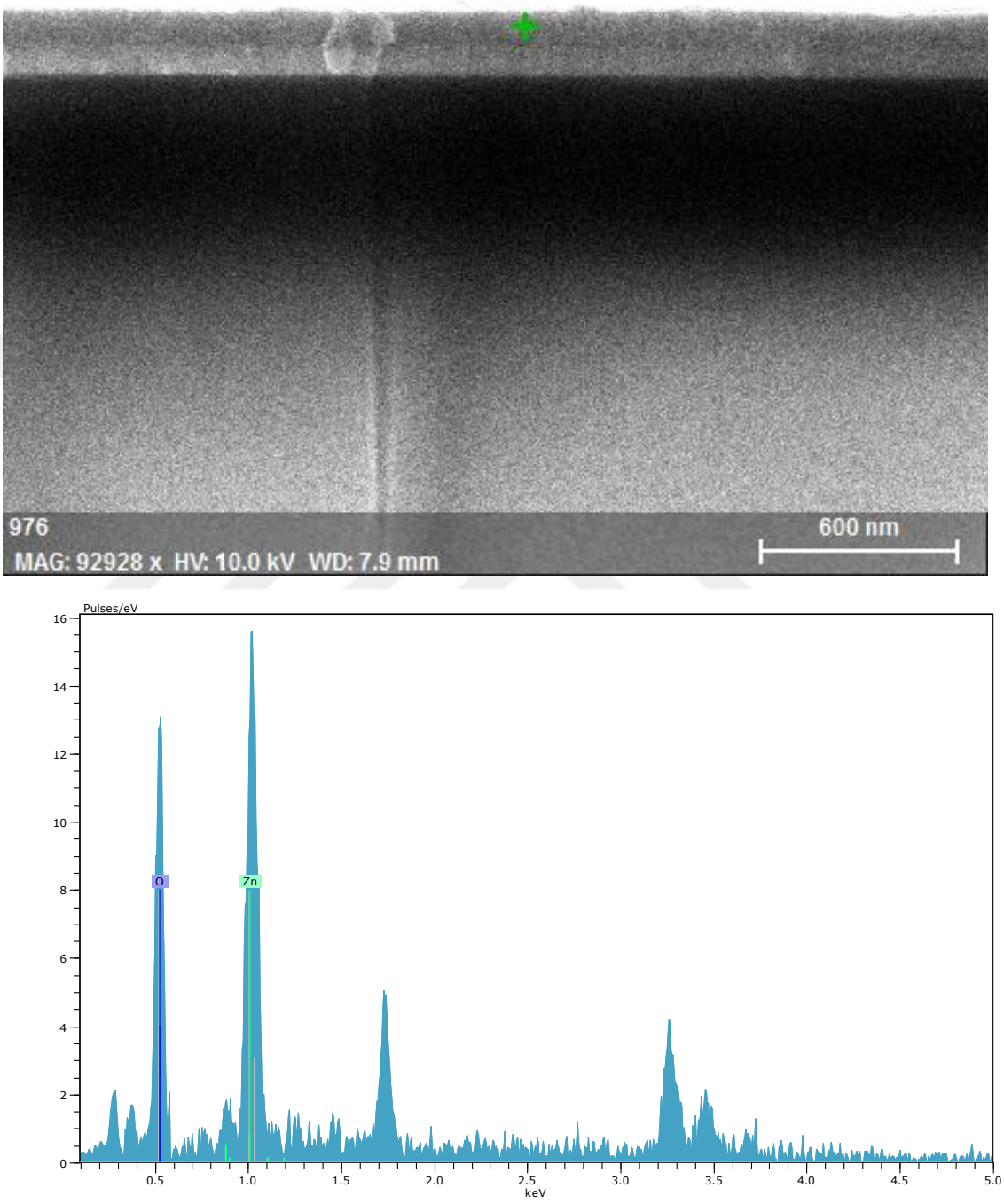

Figure A.0.2: Energy dispersive X-Ray analysis of photoelectrode

Appendix B: ROS and Calcium Measurements

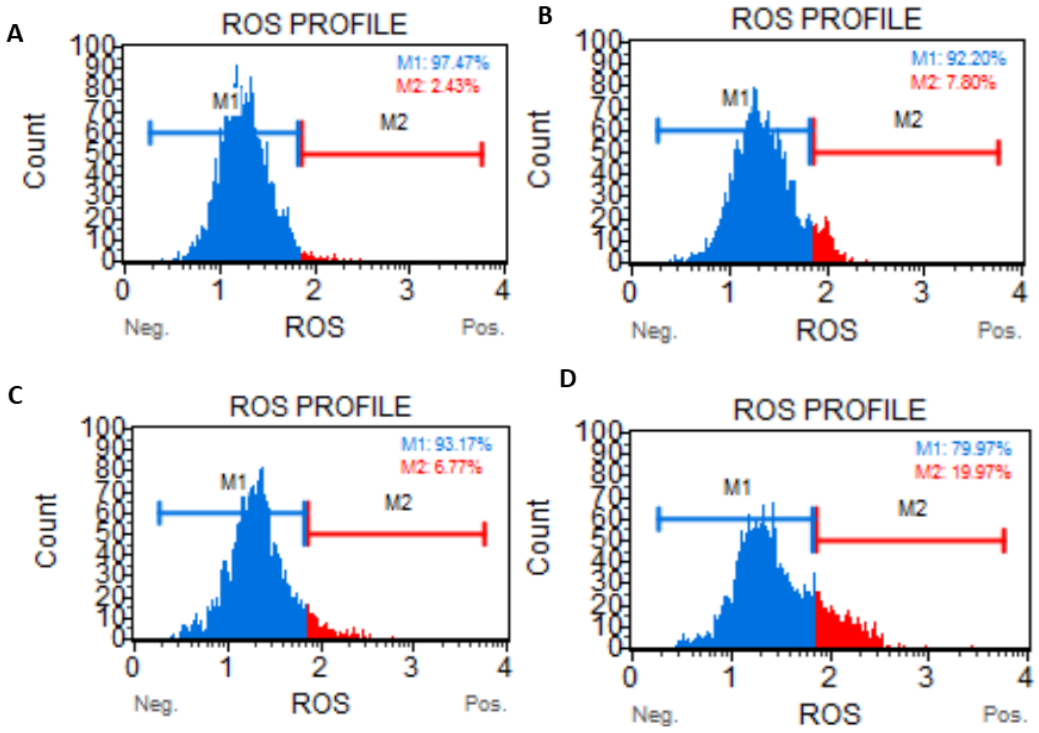

Figure B.0.1: Muse Kit Measurements of MDA-MB-231 cells A) Nontreated noncoated group B) Nontreated coated group C) Treated noncoated group and D) Treated coated group

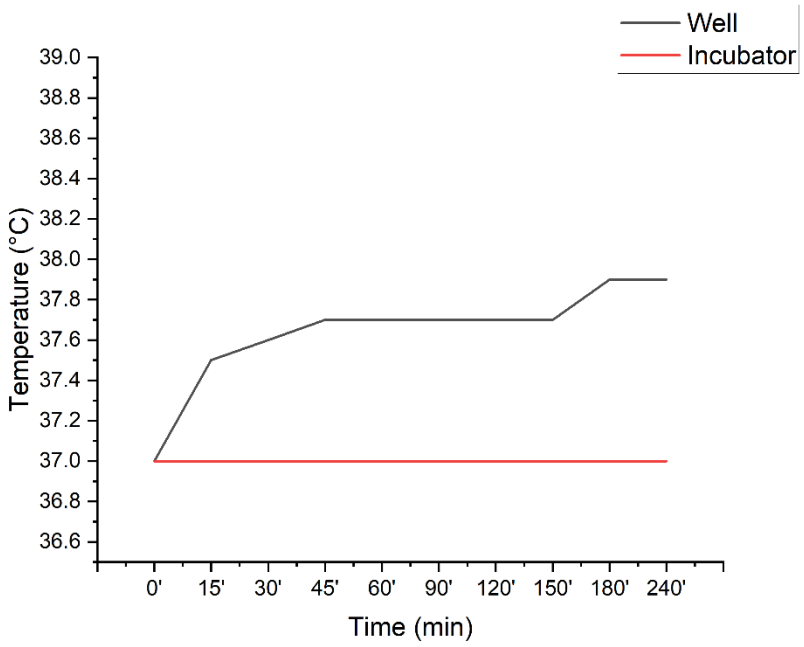

Figure B.0.2: Temperature measurements from on top of interface inside the well along 4 hours treatment

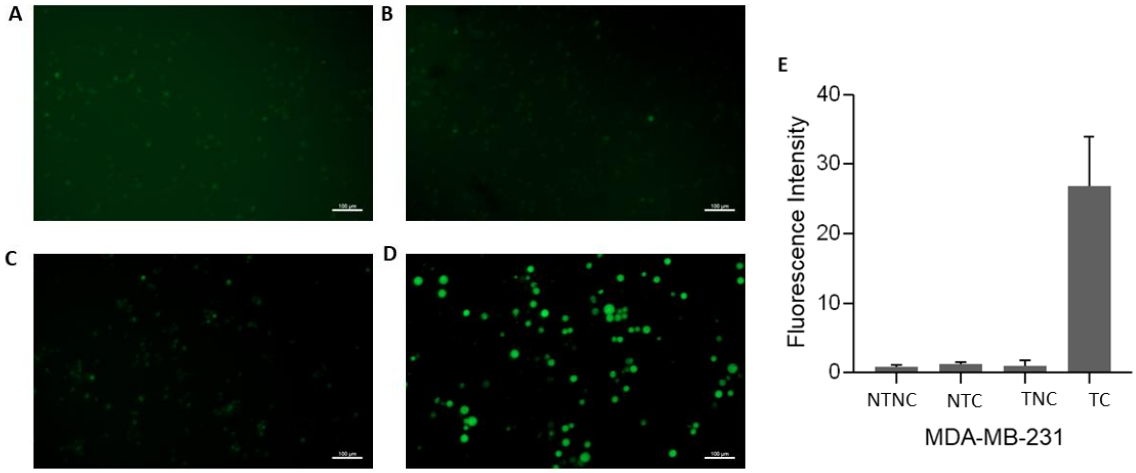

Figure B.0.3:Fluo4 AM imaging results of MDA-MB-231 cells A) nontreated noncoated group B) treated noncoated group C) nontreated coated group D) treated coated group and E) Fluorescence intensity graph of MDA-MB-231 cells

BIBLIOGRAPHY

Agostinis, P., Berg, K., Cengel, K. A., Foster, T. H., Girotti, A. W., Gollnick, S. O., Hahn, S. M., Hamblin, M. R., Juzeniene, A., Kessel, D., Korbelik, M., Moan, J., Mroz, P., Nowis, D., Piette, J., Wilson, B. C., & Golab, J. (2011). Photodynamic Therapy of Cancer: An Update. *Ca-a Cancer Journal for Clinicians*, *61*(4), 250-281. https://doi.org/10.3322/caac.20114

Alberts, B., Johnson, A., Lewis, J., Morgan, D., Raff, M., Roberts, K., & Walter, P. (2015). Molecular Biology of the Cell, Sixth Edition. *Molecular Biology of the Cell, Sixth Edition*, 1-1342. <Go to ISI>://WOS:000347857100025

Antognazza, M. R., Abdel Aziz, I., & Lodola, F. (2019). Use of Exogenous and Endogenous Photomediators as Efficient ROS Modulation Tools: Results and Perspectives for Therapeutic Purposes. *Oxidative Medicine and Cellular Longevity*, *2019*. https://doi.org/Artn 2867516
10.1155/2019/2867516

Aria, M. M. (2021). *Calcium signal modulation based on the photo electrical stimulation of voltage-gated ion channels in cancer cells enables a novel approach in cancer therapy* (Publication Number 667929) [Doctoral dissertation, Koc University]. Yükseköğretim Kurulu Başkanlığı Tez Merkezi. https://tez.yok.gov.tr/UlusalTezMerkezi/tezSorguSonucYeni.jsp

Babu, P. S. S., Manu, P. M., Dhanya, T. J., Tapas, P., Meera, R. N., Surendran, A., Aneesh, K. A., Vadakkancheril, S. J., Ramaiah, D., Nair, S. A., & Pillai, M. R. (2017). Bis(3,5-diiodo-2,4,6-trihydroxyphenyl)squaraine photodynamic therapy disrupts redox homeostasis and induce mitochondria-mediated apoptosis in human breast cancer cells. *Scientific Reports*, *7*. https://doi.org/ARTN 42126
10.1038/srep42126

Bagur, R., & Hajnoczky, G. (2017). Intracellular Ca2+ Sensing: Its Role in Calcium Homeostasis and Signaling. *Molecular Cell*, *66*(6), 780-788. https://doi.org/10.1016/j.molcel.2017.05.028

Bailey, R. (2020, 2019). *Cell Membrane Function and Structure*. https://www.thoughtco.com/cell-membrane-373364

Bareket-Keren, L., & Hanein, Y. (2014). Novel interfaces for light directed neuronal stimulation: advances and challenges. *International Journal of Nanomedicine*, *9*, 65-83. https://doi.org/10.2147/Ijn.S51193

Benfenati, V., Martino, N., Antognazza, M. R., Pistone, A., Toffanin, S., Ferroni, S., Lanzani, G., & Muccini, M. (2014). Photostimulation of Whole-Cell Conductance in Primary Rat Neocortical Astrocytes Mediated by Organic Semiconducting Thin Films. *Advanced Healthcare Materials*, *3*(3), 392-399. https://doi.org/10.1002/adhm.201300179

Berridge, M. J., Bootman, M. D., & Lipp, P. (1998). Calcium - a life and death signal. *Nature*, *395*(6703), 645-648. https://doi.org/Doi 10.1038/27094

Berzingi, S., Newman, M., & Yu, H. G. (2016). Altering bioelectricity on inhibition of human breast cancer cells. *Cancer Cell International*, *16*, 72. https://doi.org/10.1186/s12935-016-0348-8

Bezanilla, F. (2008). Ion Channels: From Conductance to Structure. *Neuron*, *60*(3), 456-468. https://doi.org/10.1016/j.neuron.2008.10.035

Binggeli, R., & Cameron, I. L. (1980). Cellular-Potentials of Normal and Cancerous Fibroblasts and Hepatocytes. *Cancer Research*, *40*(6), 1830-1835. <Go to ISI>://WOS:A1980JT99100012

Binggeli, R., & Weinstein, R. C. (1985). Deficits in elevating membrane potential of rat fibrosarcoma cells after cell contact. *Cancer Research*, *45*(1), 235-241. https://www.ncbi.nlm.nih.gov/pubmed/3965134

Boonstra, J., Mummery, C. L., Tertoolen, L. G., Van Der Saag, P. T., & De Laat, S. W. (1981). Cation transport and growth regulation in neuroblastoma cells. Modulations of K+ transport and electrical membrane properties during the cell cycle. *Journal of Cellular Physiology*, *107*(1), 75-83. https://doi.org/10.1002/jcp.1041070110

Bossio, C., Aziz, I. A., Tullii, G., Zucchetti, E., Debellis, D., Zangoli, M., Di Maria, F., Lanzani, G., & Antognazza, M. R. (2018). Photocatalytic Activity of Polymer Nanoparticles Modulates Intracellular Calcium Dynamics and Reactive Oxygen Species in HEK-293 Cells. *Frontiers in Bioengineering and Biotechnology*, *6*. https://doi.org/ARTN 114
10.3389/fbioe.2018.00114

Branton, D., & Deamer, D. W. (1972). Membrane structure. In *Membrane Structure* (pp. 1-70). Springer.

Conner, S. D., & Schmid, S. L. (2003). Regulated portals of entry into the cell. *Nature*, *422*(6927), 37-44. https://doi.org/10.1038/nature01451

Cooper, G. M., Hausman, R. E., & Hausman, R. E. (2007). *The cell: a molecular approach* (Vol. 4). ASM press Washington, DC.

Csordás, G., Madesh, M., Antonsson, B., & Hajnóczky, G. (2002). tcBid promotes Ca(2+) signal propagation to the mitochondria: control of Ca(2+) permeation through the outer mitochondrial membrane. *The EMBO journal*, *21*(9), 2198-2206. https://doi.org/10.1093/emboj/21.9.2198

D'Arcy, M. S. (2019). Cell death: a review of the major forms of apoptosis, necrosis and autophagy. *Cell Biology International*, *43*(6), 582-592. https://doi.org/10.1002/cbin.11137

Dale Purves, G. J. A., David Fitzpatrick, Lawrence C Katz, Anthony-Samuel LaMantia, James O McNamara, and S Mark Williams. (2001). *Neuroscience* (Second Edition ed.). Sinauer Associates Inc. https://www.ncbi.nlm.nih.gov/books/NBK10799/

Denac, H., Mevissen, M., & Scholtysik, G. (2000). Structure, function and pharmacology of voltage-gated sodium channels. *Naunyn-Schmiedebergs Archives of Pharmacology*, *362*(6), 453-479. https://doi.org/DOI 10.1007/s002100000319

Dent, J. A. (2010). The Evolution of Pentameric Ligand-Gated Ion Channels. *Insect Nicotinic Acetylcholine Receptors*, *683*, 11-23. https://doi.org/Book_Doi 10.1007/978-1-4419-6445-8

Di Maria, F., Lodola, F., Zucchetti, E., Benfenati, F., & Lanzani, G. (2018). The evolution of artificial light actuators in living systems: from planar to nanostructured interfaces. *Chemical Society Reviews*, *47*(13), 4757-4780. https://doi.org/10.1039/c7cs00860k

Dolphin, A. C. (2006). A short history of voltage-gated calcium channels. *British Journal of Pharmacology*, *147*, S56-S62. https://doi.org/DOI 10.1038/sj.bjp.0706442

Dougherty, T. J., Gomer, C. J., Henderson, B. W., Jori, G., Kessel, D., Korbelik, M., Moan, J., & Peng, Q. (1998). Photodynamic therapy. *Jnci-Journal of the National Cancer Institute*, *90*(12), 889-905. https://doi.org/DOI 10.1093/jnci/90.12.889

Duda, J. C., Hopkins, P. E., Shen, Y., & Gupta, M. C. (2013). Thermal transport in organic semiconducting polymers. *Applied Physics Letters*, *102*(25). https://doi.org/Artn 251912
10.1063/1.4812234
Feyen, P., Colombo, E., Endeman, D., Nova, M., Laudato, L., Martino, N., Antognazza, M. R., Lanzani, G., Benfenati, F., & Ghezzi, D. (2016). Light-evoked hyperpolarization and silencing of neurons by conjugated polymers. *Scientific Reports*, *6*. https://doi.org/ARTN 22718
10.1038/srep22718
Fleckenstein, A., Janke, J., Döring, H. J., & Leder, O. (1974). Myocardial fiber necrosis due to intracellular Ca overload-a new principle in cardiac pathophysiology. *Recent Adv Stud Cardiac Struct Metab*, *4*, 563-580.
Gautam, V., Rand, D., Hanein, Y., & Narayan, K. S. (2014). A Polymer Optoelectronic Interface Provides Visual Cues to a Blind Retina. *Advanced Materials*, *26*(11), 1751-1756. https://doi.org/10.1002/adma.201304368
Gegechkori, N., Haines, L., & Lin, J. J. (2017). Long-Term and Latent Side Effects of Specific Cancer Types. *Medical Clinics of North America*, *101*(6), 1053-+. https://doi.org/10.1016/j.mcna.2017.06.003
Ghezzi, D., Antognazza, M. R., Dal Maschio, M., Lanzarini, E., Benfenati, F., & Lanzani, G. (2011). A hybrid bioorganic interface for neuronal photoactivation. *Nature Communications*, *2*. https://doi.org/ARTN 166
10.1038/ncomms1164
Ghezzi, D., Antognazza, M. R., Maccarone, R., Bellani, S., Lanzarini, E., Martino, N., Mete, M., Pertile, G., Bisti, S., Lanzani, G., & Benfenati, F. (2013). A polymer optoelectronic interface restores light sensitivity in blind rat retinas. *Nature Photonics*, *7*(5), 400-406. https://doi.org/10.1038/Nphoton.2013.34
Giorgi, C., Baldassari, F., Bononi, A., Bonora, M., De Marchi, E., Marchi, S., Missiroli, S., Patergnani, S., Rimessi, A., Suski, J. M., Wieckowski, M. R., & Pinton, P. (2012). Mitochondrial Ca2+ and apoptosis. *Cell Calcium*, *52*(1), 36-43. https://doi.org/10.1016/j.ceca.2012.02.008
Glick, D., Barth, S., & Macleod, K. F. (2010). Autophagy: cellular and molecular mechanisms. *Journal of Pathology*, *221*(1), 3-12. https://doi.org/10.1002/path.2697
Goldman, D. E. (1943). Potential, Impedance, and Rectification in Membranes. *J Gen Physiol*, *27*(1), 37-60. https://doi.org/10.1085/jgp.27.1.37
Gouaux, E., & MacKinnon, R. (2005). Principles of selective ion transport in channels and pumps. *Science*, *310*(5753), 1461-1465. https://doi.org/10.1126/science.1113666
Gunes, S., Neugebauer, H., & Sariciftci, N. S. (2007). Conjugated polymer-based organic solar cells. *Chem Rev*, *107*(4), 1324-1338. https://doi.org/10.1021/cr050149z
Gupta, A., Shah, K., Oza, M. J., & Behl, T. (2019). Reactivation of p53 gene by MDM2 inhibitors: A novel therapy for cancer treatment. *Biomedicine & Pharmacotherapy*, *109*, 484-492. https://doi.org/10.1016/j.biopha.2018.10.155
Hajnoczky, G., Csordas, G., Madesh, M., & Pacher, P. (2000). Control of apoptosis by IP3 and ryanodine receptor driven calcium signals. *Cell Calcium*, *28*(5-6), 349-363. https://doi.org/10.1054/ceca.2000.0169
Han, M., Srivastava, S. B., Yildiz, E., Melikov, R., Surme, S., Dogru-Yuksel, I. B., Kavakli, I. H., Sahin, A., & Nizamoglu, S. (2020). Organic Photovoltaic

Pseudocapacitors for Neurostimulation. *Acs Applied Materials & Interfaces*, *12*(38), 42997-43008. https://doi.org/10.1021/acsami.0c11581

Hayman, E. G., Pierschbacher, M. D., Suzuki, S., & Ruoslahti, E. (1985). Vitronectin - a Major Cell Attachment-Promoting Protein in Fetal Bovine Serum. *Experimental Cell Research*, *160*(2), 245-258. https://doi.org/Doi 10.1016/0014-4827(85)90173-9

Higgins, S. G., Lo Fiego, A., Patrick, I., Creamer, A., & Stevens, M. M. (2020). Organic Bioelectronics: Using Highly Conjugated Polymers to Interface with Biomolecules, Cells, and Tissues in the Human Body. *Advanced Materials Technologies*, *5*(11). https://doi.org/ARTN 2000384
10.1002/admt.202000384

Hine, R. (2009). *The facts on file dictionary of biology*. Infobase Publishing.

Hodgkin, A. L., & Katz, B. (1949). The effect of sodium ions on the electrical activity of giant axon of the squid. *J Physiol*, *108*(1), 37-77. https://doi.org/10.1113/jphysiol.1949.sp004310

Horn, A., & Jaiswal, J. K. (2019). Structural and signaling role of lipids in plasma membrane repair. *Plasma Membrane Repair*, *84*, 67-98. https://doi.org/10.1016/bs.ctm.2019.07.001

Hoyer-Hansen, M., Bastholm, L., Szyniarowski, P., Campanella, M., Szabadkai, G., Farkas, T., Bianchi, K., Fehrenbacher, N., Elling, F., Rizzuto, R., Mathiasen, I. S., & Jaattela, M. (2007). Control of macroautophagy by calcium, calmodulin-dependent kinase kinase-beta, and Bcl-2. *Molecular Cell*, *25*(2), 193-205. https://doi.org/10.1016/j.molcel.2006.12.009

Hsiao, Y. S., Liao, Y. H., Chen, H. L., Chen, P., & Chen, F. C. (2016). Organic Photovoltaics and Bioelectrodes Providing Electrical Stimulation for PC12 Cell Differentiation and Neurite Outgrowth. *ACS Appl Mater Interfaces*, *8*(14), 9275-9284. https://doi.org/10.1021/acsami.6b00916

Hucho, F., & Weise, C. (2001). Ligand-gated ion channels. *Angewandte Chemie-International Edition*, *40*(17), 3101-3116. <Go to ISI>://WOS:000170901400001

Iftinca, M., Mckay, B. E., Snutch, T. P., McRory, J. E., Turner, R. W., & Zamponi, G. W. (2006). Temperature dependence of T-type calcium channel gating. *Neuroscience*, *142*(4), 1031-1042. https://doi.org/10.1016/j.neuroscience.2006.07.010

Isom, L. L., De Jongh, K. S., & Catterall, W. A. (1994). Auxiliary subunits of voltage-gated ion channels. *Neuron*, *12*(6), 1183-1194. https://doi.org/10.1016/0896-6273(94)90436-7

Janigro, D., Perju, C., Fazio, V., Hallene, K., Dini, G., Agarwal, M. K., & Cucullo, L. (2006). Alternating current electrical stimulation enhanced chemotherapy: a novel strategy to bypass multidrug resistance in tumor cells. *Bmc Cancer*, *6*. https://doi.org/Artn 72
10.1186/1471-2407-6-72

Johnstone, B. M. (1959). Micro-electrode penetration of ascites tumour cells. *Nature*, *183*(4658), 411. https://doi.org/10.1038/183411a0

Josselyn, S. A. (2018). The past, present and future of light-gated ion channels and optogenetics. *Elife*, *7*. https://doi.org/ARTN e42367
10.7554/eLife.42367

Kang, J., Huguenard, J. R., & Prince, D. A. (2000). Voltage-gated potassium channels activated during action potentials in layer V neocortical pyramidal neurons.

Journal of Neurophysiology, *83*(1), 70-80. https://doi.org/DOI 10.1152/jn.2000.83.1.70

Kelekar, A. (2005). Autophagy. *Cell Injury: Mechanisms, Responses, and Repair*, *1066*, 259-271. https://doi.org/10.1196/annals.1363.015

Kleinman, H. K., Luckenbilledds, L., Cannon, F. W., & Sephel, G. C. (1987). Use of Extracellular-Matrix Components for Cell-Culture. *Analytical Biochemistry*, *166*(1), 1-13. https://doi.org/Doi 10.1016/0003-2697(87)90538-0

Lester, H. A., Krouse, M. E., Nass, M. M., Wassermann, N. H., & Erlanger, B. F. (1980). Covalently Bound Photoisomerizable Agonist - Comparison with Reversibly Bound Agonists at Electrophorus Electroplaques. *Journal of General Physiology*, *75*(2), 207-232. https://doi.org/DOI 10.1085/jgp.75.2.207

Li, J., Guo, C. R., Wang, Z. S., Gao, K., Shi, X. D., & Liu, J. (2016). Electrical stimulation towards melanoma therapy via liquid metal printed electronics on skin. *Clinical and Translational Medicine*, *5*. https://doi.org/ARTN 21 10.1186/s40169-016-0102-9

Li, X. S., Lovell, J. F., Yoon, J., & Chen, X. Y. (2020). Clinical development and potential of photothermal and photodynamic therapies for cancer. *Nature Reviews Clinical Oncology*, *17*(11), 657-674. https://doi.org/10.1038/s41571-020-0410-2

Lodola, F., Martino, N., Tullii, G., Lanzani, G., & Antognazza, M. R. (2017). Conjugated polymers mediate effective activation of the Mammalian Ion Channel Transient Receptor Potential Vanilloid 1. *Sci Rep*, *7*(1), 8477. https://doi.org/10.1038/s41598-017-08541-6

Loschwitz, J., Olubiyi, O. O., Hub, J. S., Strodel, B., & Poojari, C. S. (2020). Computer simulations of protein-membrane systems. *Computational Approaches for Understanding Dynamical Systems: Protein Folding and Assembly*, *170*, 273-403. https://doi.org/10.1016/bs.pmbts.2020.01.001

Lyman, G. H. (2009). Impact of chemotherapy dose intensity on cancer patient outcomes. *J Natl Compr Canc Netw*, *7*(1), 99-108. https://doi.org/10.6004/jnccn.2009.0009

Lymangrover, J., Pearlmutter, A. F., Franco-Saenz, R., & Saffran, M. (1975). Transmembrane potentials and steroidogenesis in normal and neoplastic human adrenocortical tissue. *J Clin Endocrinol Metab*, *41*(4), 697-706. https://doi.org/10.1210/jcem-41-4-697

Macfarlane, S. N., & Sontheimer, H. (2000). Changes in ion channel expression accompany cell cycle progression of spinal cord astrocytes. *Glia*, *30*(1), 39-48. https://doi.org/Doi 10.1002/(Sici)1098-1136(200003)30:1<39::Aid-Glia5>3.0.Co;2-S

Malhotra, V., & Perry, M. C. (2003). Classical Chemotherapy: Mechanisms, Toxicities and the Therapeutc Window. *Cancer Biology & Therapy*, *2*(sup1), 1-3. https://doi.org/10.4161/cbt.199

Malumbres, M., & Barbacid, M. (2009). Cell cycle, CDKs and cancer: a changing paradigm. *Nat Rev Cancer*, *9*(3), 153-166. https://doi.org/10.1038/nrc2602

Marban, E., Yamagishi, T., & Tomaselli, G. F. (1998). Structure and function of voltage-gated sodium channels. *Journal of Physiology-London*, *508*(3), 647-657. https://doi.org/DOI 10.1111/j.1469-7793.1998.647bp.x

Marino, A. A., Morris, D. M., Schwalke, M. A., Iliev, I. G., & Rogers, S. (1994). Electrical Potential Measurements in Human Breast-Cancer and Benign Lesions. *Tumor Biology*, *15*(3), 147-152. <Go to ISI>://WOS:A1994PF74900004

Mathew, R., Karantza-Wadsworth, V., & White, E. (2007). Role of autophagy in cancer. *Nat Rev Cancer*, *7*(12), 961-967. https://doi.org/10.1038/nrc2254

Mazia, D., Schatten, G., & Sale, W. (1975). Adhesion of cells to surfaces coated with polylysine. Applications to electron microscopy. *J Cell Biol*, *66*(1), 198-200. https://doi.org/10.1083/jcb.66.1.198

Melczer, N., & Kiss, J. (1957). Electrical method for detection of early cancerous growth of the skin. *Nature*, *179*(4571), 1177-1179. https://doi.org/10.1038/1791177b0

Negri, S., Faris, P., Rosti, V., Antognazza, M. R., Lodola, F., & Moccia, F. (2020). Endothelial TRPV1 as an Emerging Molecular Target to Promote Therapeutic Angiogenesis. *Cells*, *9*(6). https://doi.org/ARTN 1341
10.3390/cells9061341

Norberg, E., Gogvadze, V., Ott, M., Horn, M., Uhlén, P., Orrenius, S., & Zhivotovsky, B. (2008). An increase in intracellular Ca2+ is required for the activation of mitochondrial calpain to release AIF during cell death. *Cell Death & Differentiation*, *15*(12), 1857-1864. https://doi.org/10.1038/cdd.2008.123

Orr, C. W., Yoshikawa-Fukada, M., & Ebert, J. D. (1972). Potassium: effect on DNA synthesis and multiplication of baby-hamster kidney cells: (cell cycle-membrane potential-synchronization-transformation). *Proc Natl Acad Sci U S A*, *69*(1), 243-247. https://doi.org/10.1073/pnas.69.1.243

Owusu-Ansah, E., Yavari, A., & Banerjee, U. (2008). A protocol for in vivo detection of reactive oxygen species.

Pacher, P., & Hajnoczky, G. (2001). Propagation of the apoptotic signal by mitochondrial waves. *Embo Journal*, *20*(15), 4107-4121. https://doi.org/DOI 10.1093/emboj/20.15.4107

Perazella, M. A. (2012). Onco-Nephrology: Renal Toxicities of Chemotherapeutic Agents. *Clinical Journal of the American Society of Nephrology*, *7*(10), 1713-1721. https://doi.org/10.2215/Cjn.02780312

Phan, N. N., Wang, C. Y., Chen, C. F., Sun, Z. D., Lai, M. D., & Lin, Y. C. (2017). Voltage-gated calcium channels: Novel targets for cancer therapy. *Oncology Letters*, *14*(2), 2059-2074. https://doi.org/10.3892/ol.2017.6457

Pongs, O. (1999). Voltage-gated potassium channels: from hyperexcitability to excitement. *Febs Letters*, *452*(1-2), 31-35. https://doi.org/Doi 10.1016/S0014-5793(99)00535-9

Proskuryakov, S. Y., Konoplyannikov, A. G., & Gabai, V. L. (2003). Necrosis: a specific form of programmed cell death? *Experimental Cell Research*, *283*(1), 1-16. https://doi.org/10.1016/S0014-4827(02)00027-7

Rao, V. R., Perez-Neut, M., Kaja, S., & Gentile, S. (2015). Voltage-Gated Ion Channels in Cancer Cell Proliferation. *Cancers*, *7*(2), 849-875. https://doi.org/10.3390/cancers7020813

Redmann, K., Muller, V., Tanneberger, S., & Kalkoff, W. (1972). The membrane potential of primary ovarian tumor cells in vitro and its dependence on the cell cycle. *Acta Biol Med Ger*, *28*(5), 853-856. https://www.ncbi.nlm.nih.gov/pubmed/5074152

Reece, J. B., & Campbell, N. A. (2011). *Campbell biology* (9th ed.). Benjamin Cummings / Pearson.

Reubish, D. S., Emerling, D. E., DeFalco, J., Steiger, D., Victoria, C. L., & Vincent, F. (2009). Functional assessment of temperature-gated ion-channel activity using a

real-time PCR machine. *Biotechniques*, *47*(3), Iii-Viii. https://doi.org/10.2144/000113198

Ruiz, M. D., & Kraus, R. L. (2015). Voltage-Gated Sodium Channels: Structure, Function, Pharmacology, and Clinical Indications. *Journal of Medicinal Chemistry*, *58*(18), 7093-7118. https://doi.org/10.1021/jm501981g

Sachs, H. G., Stambrook, P. J., & Ebert, J. D. (1974). Changes in membrane potential during the cell cycle. *Experimental Cell Research*, *83*(2), 362-366. https://doi.org/10.1016/0014-4827(74)90350-4

Schafer, K. A. (1998). The cell cycle: A review. *Veterinary Pathology*, *35*(6), 461-478. https://doi.org/Doi 10.1177/030098589803500601

Shakeri, R., Kheirollahi, A., & Davoodi, J. (2017). Apaf-1: Regulation and function in cell death. *Biochimie*, *135*, 111-125. https://doi.org/10.1016/j.biochi.2017.02.001

Shevchenko, A., & Simons, K. (2010). Lipidomics: coming to grips with lipid diversity. *Nature Reviews Molecular Cell Biology*, *11*(8), 593-598. https://doi.org/10.1038/nrm2934

Simms, B. A., & Zamponi, G. W. (2014). Neuronal Voltage-Gated Calcium Channels: Structure, Function, and Dysfunction. *Neuron*, *82*(1), 24-45. https://doi.org/10.1016/j.neuron.2014.03.016

Singh, R., Letai, A., & Sarosiek, K. (2019). Regulation of apoptosis in health and disease: the balancing act of BCL-2 family proteins. *Nature Reviews Molecular Cell Biology*, *20*(3), 175-193. https://doi.org/10.1038/s41580-018-0089-8

Stevenson, D., Binggeli, R., Weinstein, R. C., Keck, J. G., Lai, M. C., & Tong, M. J. (1989). Relationship between Cell-Membrane Potential and Natural-Killer Cell Cytolysis in Human Hepatocellular-Carcinoma Cells. *Cancer Research*, *49*(17), 4842-4845. <Go to ISI>://WOS:A1989AL76000030

Strobl, J. S., Wonderlin, W. F., & Flynn, D. C. (1995). Mitogenic signal transduction in human breast cancer cells. *General Pharmacology*, *26*(8), 1643-1649. https://doi.org/Doi 10.1016/0306-3623(95)00062-3

Szabo, C. (2005). Mechanisms of cell necrosis. *Critical Care Medicine*, *33*(12 Suppl), S530-534. https://doi.org/10.1097/01.ccm.0000187002.88999.cf

Tokuoka, S., & Morioka, H. (1957). The membrane potential of the human cancer and related cells. I. *Gan*, *48*(4), 353-354. https://www.ncbi.nlm.nih.gov/pubmed/13524400

Tullii, G., Desii, A., Bossio, C., Bellani, S., Colombo, M., Martino, N., Antognazza, M. R., & Lanzani, G. (2017). Bimodal functioning of a mesoporous, light sensitive polymer/electrolyte interface. *Organic Electronics*, *46*, 88-98. https://doi.org/10.1016/j.orgel.2017.04.007

Vargas-Estevez, C., Blanquer, A., Murillo, G., Duque, M., Barrios, L., Nogues, C., Ibanez, E., & Esteve, J. (2018). Electrical stimulation of cells through photovoltaic microcell arrays. *Nano Energy*, *51*, 571-578. https://doi.org/10.1016/j.nanoen.2018.07.012

Vousden, K. H., & Lu, X. (2002). Live or let die: the cell's response to p53. *Nat Rev Cancer*, *2*(8), 594-604. https://doi.org/10.1038/nrc864

Wang, Y. N., Hu, S. M., Tuerdi, M., Yu, X. M., Zhang, H. S., Zhou, Y. Z., Cao, J., Vaz, I. D., & Zhou, J. L. (2020). Initiator and executioner caspases in salivary gland apoptosis of Rhipicephalus haemaphysaloides. *Parasites & Vectors*, *13*(1). https://doi.org/10.1186/s13071-020-04164-5

Whitaker, M., & Patel, R. (1990). Calcium and Cell-Cycle Control. *Development*, *108*(4), 525-542. <Go to ISI>://WOS:A1990DB48900002

Wood, J. N., Boorman, J. P., Okuse, K., & Baker, M. D. (2004). Voltage-gated sodium channels and pain pathways. *Journal of Neurobiology*, *61*(1), 55-71. https://doi.org/10.1002/neu.20094

Woodrough, R. E., Canti, G., & Watson, B. W. (1975). Electrical potential difference between basal cell carcinoma, benign inflammatory lesions and normal tissue. *Br J Dermatol*, *92*(1), 1-7. https://www.ncbi.nlm.nih.gov/pubmed/1156538

Wulff, H., Castle, N. A., & Pardo, L. A. (2009). Voltage-gated potassium channels as therapeutic targets. *Nature Reviews Drug Discovery*, *8*(12), 982-1001. https://doi.org/10.1038/nrd2983

Xu, G. W., & Shi, Y. F. (2007). Apoptosis signaling pathways and lymphocyte homeostasis. *Cell Research*, *17*(9), 759-771. https://doi.org/10.1038/cr.2007.52

Yang, M., & Brackenbury, W. J. (2013). Membrane potential and cancer progression. *Frontiers in Physiology*, *4*, 185. https://doi.org/10.3389/fphys.2013.00185

Yu, F. H., & Catterall, W. A. (2003). Overview of the voltage-gated sodium channel family. *Genome Biol*, *4*(3), 207. https://doi.org/10.1186/gb-2003-4-3-207

Zamponi, G. W., Striessnig, J., Koschak, A., & Dolphin, A. C. (2015). The Physiology, Pathology, and Pharmacology of Voltage-Gated Calcium Channels and Their Future Therapeutic Potential. *Pharmacological Reviews*, *67*(4), 821-870. https://doi.org/10.1124/pr.114.009654

Zhi, D. F., Yang, T., O'hagan, J., Zhang, S. B., & Donnelly, R. F. (2020). Photothermal therapy. *Journal of Controlled Release*, *325*, 52-71. https://doi.org/10.1016/j.jconrel.2020.06.032